UNIVERSITÀ DEGLI STUDI DI PADOVA

DIPARTIMENTO DI BIOLOGIA

Corso di Laurea magistrale in Biologia Evoluzionistica

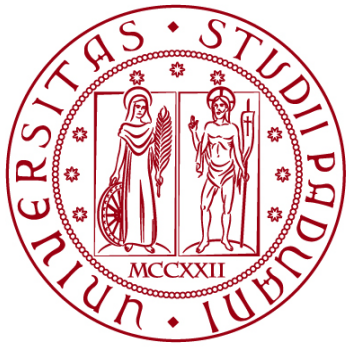

TESI DI LAUREA

PHYSIOLOGICAL RESPONSES OF DESERT SOIL MICROALGAE TO ENVIRONMENTAL STRESSES: A PHOTOBIOREACTOR STUDY

Relatore: Prof. Francesco Dal Grande
Dipartimento di Biologia

Correlatore: Dott.ssa Veronica Malavasi
Centro di Ateneo Orto Botanico
Dott. Giorgio Perin
Dipartimento di Biologia

Laureanda: Laura Fortin

ANNO ACCADEMICO 2024/2025

CONTENTS

ABSTRACT 3
Riassunto 4
1 INTRODUCTION 5
1.1 Drylands area 5
1.2 Extremophile microalgae 6
1.3 Microalgae and bioeconomy 8
1.4 Cyanobacteria 9
1.5 Industrial production systems 11
1.6 Open raceway ponds 11
1.7 Photobioreactors (PBR) 12
2 THESIS OBJECTIVES 15
3 MATERIAL E METHODS 17
3.1 BIODESERT 17
3.2 Algae inoculum establishment 18
3.3 BBM+C 18
3.4 First photobioreactor experiment 20
3.5 Growth monitoring 21
3.6 Sample dilution 21
3.7 Second photobioreactor experiment 22
3.8 Culture establishment with samples of soil 22
3.9 Inoculum establishment with samples of soil 23
3.10 Growth monitoring 24
3.11 Sample dilution and introduction of water bath 25
3.12 Nutrient enrichment of the medium 25
3.13 Preparation of stock solutions of $NaNO_3$, KH_2PO_4, K_2HPO_4 26
3.14 Semicontinuous dilutions and biomass calculation 31
3.14.1 Semicontinuous dilutions 31
3.14.2 Calculation of biomass before and after dilution 31
3.15 Photoperiod setup 33
3.16 Preparation of samples for absorbance measurement 33
3.17 Sample preparation for DNA extraction 34
3.18 Absorbance curve measurement 35
3.19 DNA extraction 37

4 RESULTS AND DISCUSSION 39
4.1 Growth dynamics under stress conditions 39
4.2 Culture observations 41
4.3 Monitoring status of culture in the second experiment 42
4.4 Culture observations 43
4.5 Microscopic observations 44
4.5.1 Intermediate phase of the experiment 44
4.5.2 Final phase of the experiment 45
4.6 Pigment analysis 46
4.7 Analysis of DNA extraction 50
5 CONCLUSION 51
6 BIBLIOGRAFY 53
7 APPENDIX 55
RINGRAZIAMENTI 63

ABSTRACT

Arid lands are characterized by low soil water content, with an aridity index (AI) below 0.65, covering approximately 41% of the Earth's surface. Despite being considered extreme environments, these regions host a rich microbial biodiversity, including fungi, algae, bacteria, bryophytes and cyanobacteria. The increasing global temperatures due to climate change are exacerbating aridification leading to a decline in microbial communities. This study focuses on continuing the BIODESERT project by identifying and analyzing desert microalgae cultivated in fourteen soil samples.

An algal photobioreactor was employed to monitor the cultures, simulating an industrial growth environment. This approach facilitates the selection of microalgae for their ability to grow in extreme conditions, which will optimize biomass production and decrease contamination risks.

Key parameters such as pH, light intensity, and temperature were monitored. In particular, the growth trend was assessed through repeated spectrophotometer measurements. Subsequently, samples were collected for DNA extraction using "Quick-DNA Fecal/Soil Microbe Microprep" kit.

Despite the significant microbial diversity in arid soils, knowledge remains limited, therefore this study represents a preliminary screening aimed at characterizing microalgal biodiversity adapted to desertified areas and to better understand which, among the species are more resilience than others to environmental stressors. Future applications include potential industrial biotechnological uses, for example in cosmetics, food, and animal feed fields. Moreover, the presence of carotenoids in these microalgae may contribute to human health by counteracting oxidative stress and preventing the effects of free radicals. These compounds are important for their antioxidant, anti-aging, anti-inflammatory, antiangiogenic, cardioprotective, and hepatoprotective properties. The findings of this study will be a first step to carrying out more in-depth studies in the future.

Riassunto

Le terre aride sono caratterizzate da un basso contenuto idrico del suolo, con un indice di aridità (AI) inferiore a 0,65, e coprono circa il 41% della superficie terrestre. Nonostante siano considerate ambienti estremi, queste regioni ospitano una ricca biodiversità microbica, comprendente funghi, alghe, batteri, briofite e cianobatteri. L'aumento delle temperature globali dovuto ai cambiamenti climatici sta intensificando i processi di aridificazione, portando a un declino delle comunità microbiche. Questo studio si inserisce nella continuazione del progetto BIODESERT e ha come obiettivo l'identificazione e l'analisi di microalghe desertiche coltivate a partire da quattordici campioni di suolo.

Per monitorare le colture è stato impiegato un fotobioreattore algale, in grado di simulare un ambiente di crescita industriale. Questo approccio consente di selezionare le microalghe sulla base della loro capacità di crescere in condizioni estreme, ottimizzando così la produzione di biomassa e riducendo i rischi di contaminazione.

Sono stati monitorati parametri chiave come pH, intensità luminosa e temperatura. In particolare, l'andamento della crescita è stato valutato tramite misurazioni spettrofotometriche ripetute. Successivamente, i campioni sono stati raccolti per l'estrazione del DNA utilizzando il kit *Quick-DNA Fecal/Soil Microbe Microprep*.

Nonostante l'elevata diversità microbica presente nei suoli aridi, le conoscenze restano limitate. Questo studio rappresenta quindi uno screening preliminare volto a caratterizzare la biodiversità microalgale adattata alle aree desertificate e a comprendere meglio quali specie risultino più resilienti agli stress ambientali. Le applicazioni future includono potenziali usi industriali in campo biotecnologico, ad esempio nei settori cosmetico, alimentare e mangimistico. Inoltre, la presenza di carotenoidi in queste microalghe potrebbe apportare benefici alla salute umana contrastando lo stress ossidativo e prevenendo gli effetti dei radicali liberi. Questi composti sono noti per le loro proprietà antiossidanti, anti-invecchiamento, antinfiammatorie, antiangiogeniche, cardioprotettive ed epatoprotettive. I risultati di questo studio rappresentano un primo passo per lo sviluppo di ricerche più approfondite in futuro.

1 INTRODUCTION

1.1 Drylands area

Climate change is a major driver of biodiversity loss from local to global scales, in both terrestrial and aquatic ecosystems. Given the dependence of crucial ecosystem processes and services on biodiversity, climate-change-driven biodiversity losses will dramatically alter the functioning of natural ecosystems. Key ecosystem processes such as nutrient cycling, carbon sequestration, and organic matter decomposition depend on soil bacteria and fungi (Maestre et al., 2015)

Climate change has a particular impact on drylands that represent environments characterized by extremely low annual precipitation (below 50 mm), absence of plant cover, and soils with minimal organic matter (Scortino 2021). Drylands, defined by an aridity index below 0.65, cover 41% of the terrestrial surface and include 35% of global biodiversity and 20% of plant diversity hotspots (Fig. 1).

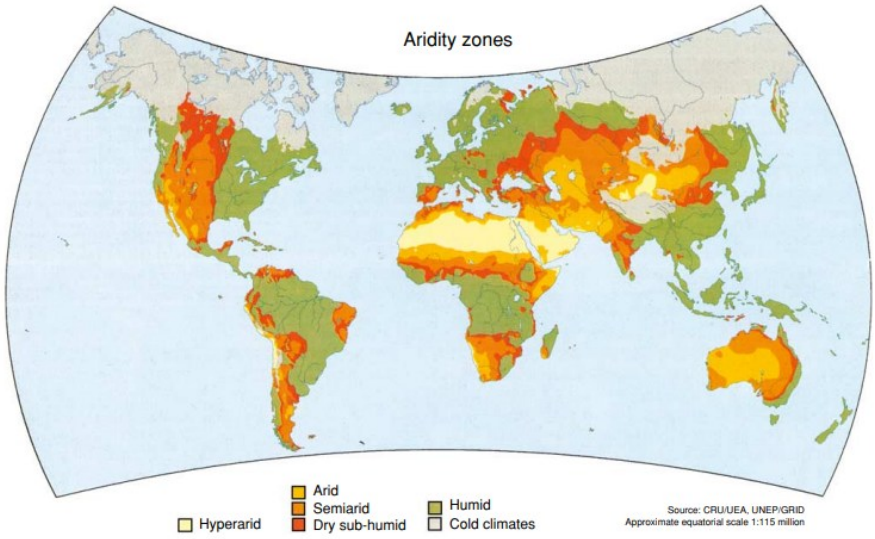

Fig. 1: Aridity zones of the world (Belnap 2005).

Drylands are classified according to the aridity index (AI) as follows: hyperarid (AI < 0.05), arid (0.05 < AI < 0.20), semiarid (0.20 < AI < 0.50) and dry subhumid (0.50 < AI < 0.65) areas, which occupy 6.6%, 10.6%, 15.2%, and 8.7%, of global land area respectively (Maestre et al., 2021). From an

ecological perspective, deserts represent critical thresholds of resource degradation for subsistence of human life.

Drylands are expected to expand in global area by 11–23% by 2100, experiencing increased aridity and reduced soil moisture. Land degradation and desertification already affect ~250 million people in the developing world (Maestre et al., 2015).

Because the provisioning of ecosystem services essential for human development (soil fertility, food, and biomass production) heavily relies on the abundance, composition, and diversity of soil fungi and bacteria, it is crucial to understand how changes in aridity affect soil microbial communities. Studying these communities is a way to better understand resilience and ecosystem services in arid environments and to assess potential yet unexplored applications (Maestre et al., 2015).

1.2 Extremophile microalgae

Microalgae are an extremely diverse group of microscopic organisms found in nearly all ecosystems on Earth, including marine and freshwater environments, desert sands, hot springs, as well as snow and ice (Malavasi et al., 2020). As photosynthetic organisms, they can harness solar energy to convert water and carbon dioxide into biomass.

Living in a desert presents an enormous challenge for photosynthetic organisms. These environments are dry, experience extreme temperatures, and expose their inhabitants to intense solar radiation during periods of time when the potential for dissipating absorbed energy through photo-synthetic activity is limited by temperature or the lack of water. Despite these stresses, many desert regions contain a tremendous diversity of microscopic life, much of which is organized into a biological crust at the soil surface (bryophytes, lichens, fungi, and unicellular green algae). (Gray et al., 2007).

Extremophile organisms may be divided into two broad categories: extremophilic organisms that require one or more harsh conditions to grow, and extremotolerant ones that can sustain very high values of one or more physicochemical parameters, while growing optimally under normal conditions (Malavasi et al., 2020).

In the last decade, attention to extreme environments has increased because of interests to isolate previously unknown extremophilic microorganisms in pure culture and to profile their metabolites. Microorganisms that live in extreme environments produce extremozymes and extremolytes, potentially valuable resources for the development of a bio-based economy through their application in biotechnologies (Raddadi et al., 2015). Microalgae can endure extreme environmental conditions like anoxia, temperature variations, and high UV radiation. Their high photosynthetic efficiency, the large number of byproducts within the cells, and the advantages compared to food and feed crop cultivation make them an important candidate for food industries. Certain specifications, including environmental and system conditions, are required for proper growth (Barboza-Rodríguez, R et al., 2024).

The exploitation of microalgae biomass as a source of energy and materials could provide a valuable contribution, thanks to these organisms' high efficiency in the fixation of carbon dioxide via photosynthesis. Algae cultivation can also be combined with wastewater treatment or with the sustainable production of valuable molecules (such as pigments and food additives) that, coupled with energy production, could enhance overall environmental benefits and the economic balance. The industrial exploitation of algae biomass thus requires efforts in strains improvement or domestication, as well as the selection of specific genetic features that are advantageous for the cultivation in intensive conditions (Perin et al., 2017) (Fig. 2).

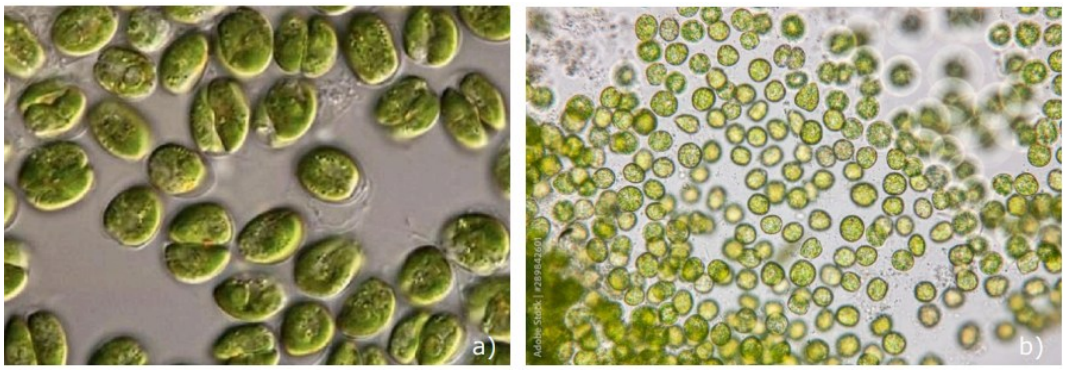

Fig. 2: Some of the most produced microalgae species: a) Chlorella spp.; *b) Nannochloropsis oculata (Vazquez et al., 2022).*

Desert microalgae identification is not merely a taxonomic exercise, but it's important to study because they are ideal models for understanding the limits of photosynthesis and life under extreme conditions; in a world facing increasing desertification they can contribute to carbon sequestration, soil stabilization, and the maintenance of biogeochemical cycles; finally, some of them produce metabolites with high biotechnological potential (antioxidants, pigments, bioactive molecules).

1.3 Microalgae and bioeconomy

The microalgae sector is emerging and making a major contribution to the global bioeconomy, producing biomass useful for applications related to human consumption, such as cosmetic pharmaceuticals, food, and feed (Malchira et al., 2019) (Fig. 3).

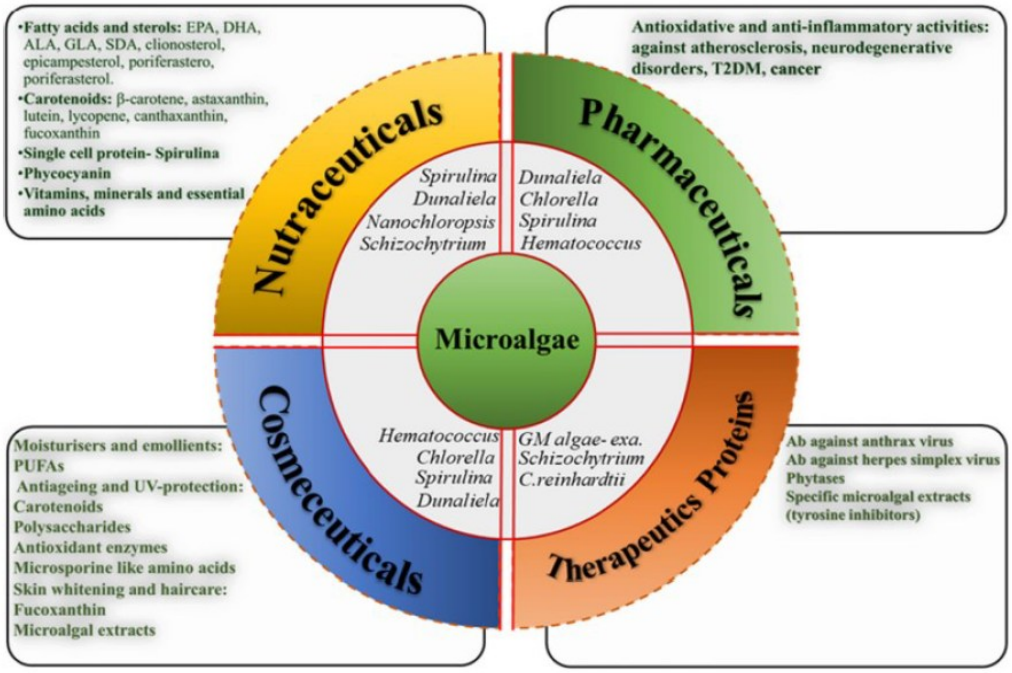

Fig. 3: Industrial applications of microalgae (Malchira et al., 2019).

The integration of microalgae into various food formulations has contributed to a significant increase in microalgal products' availability on the market. (Lafarga et al., 2020). However, their contribution to the bioeconomy would

be significantly greater if the current production capacity could be expanded and new applications of commercial interest are developed. Until now, microalgae have been proposed as a source to produce biofuels, chemical- and bio-fertilizers, but they can also provide services such as waste water treatment and waste gas cleaning (Fernández et al., 2021).

Despite the potential contribution of microalgae to renewable energies and the market, there is still a lack of comprehensive and solid knowledge base on their ability to survive and being possibly exploited (European Commission et al. 2022).

1.4 Cyanobacteria

Cyanobacteria are Gram-negative bacteria, with sizes ranging from 0.2 to 5 µm, they can exist as solitary cells or in colonies (Pasqua et al.,2019). They are characterized by their ability to perform oxygenic photosynthesis.

For this reason, they are generally classified as microalgae (Pasqua et al., 2019). These play an important role in nature as primary producers of organic matter, using light as energy source, water as electron donor and CO_2 as carbon source. Oxygen photosynthesis reactions are used to drive biosynthesis at the expense of inorganic nutrients (Zuccaro et al., 2019).

Cyanobacteria are found in every environment on Earth, from oceans to freshwater and soil, in Arctic regions, hot and cold deserts, and thermal springs. They are also present in conditions that are particularly challenging for eukaryotes, as they possess high adaptability and remarkable survival capabilities (Pasqua et al., 2019).

Cyanobacteria are members of the biological crust community that have demonstrated important functions in soil. They are pioneers in the process of soil stabilization and increase microtopographical roughness, containing erosion by water and wind. Furthermore, cyanobacteria improve water availability and soil stability through the filamentous morphology of some genera and the exopolysaccharides they excrete (Roncero-Ramos et al., 2019).

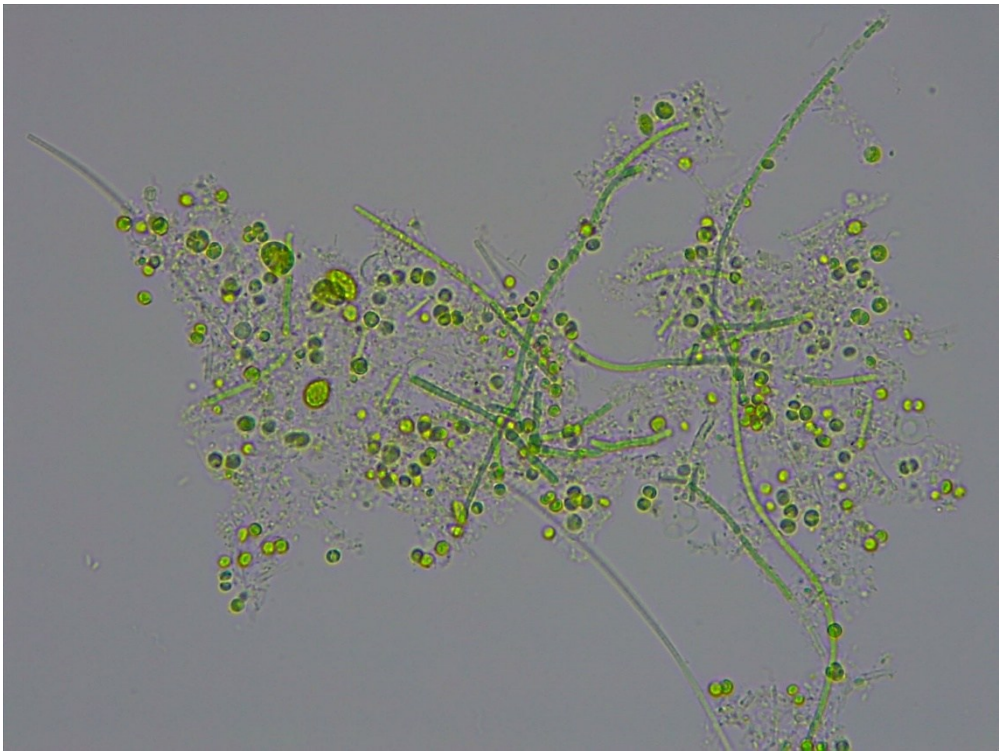

Fig. 4: Microscope observation of Cyanobacteria (elongated cells) and microalgae (round cells) (20x).

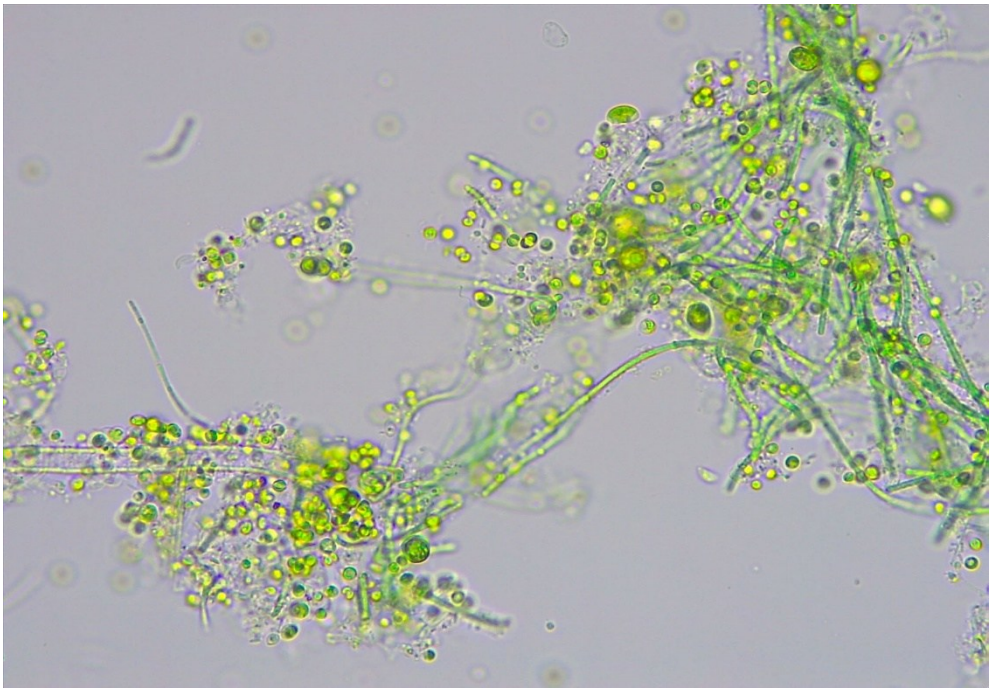

Fig. 5: Microscope observation of Cyanobacteria (elongated cells) and microalgae (round cells) (40x).

1.5 Industrial production systems

The main factors that regulate the growth and cultivation of microalgae are light, CO_2 availability, nutrients, process parameters (pH, temperature), and especially the type of system used for the cultivation (Ahmad et al., 2021).

For biotechnological applications, microalgae are mainly cultivated in closed photobioreactors (PBR) and open systems (raceway ponds).

In this study, a photobioreactor was employed, and the comparison between the two biotechnological applications used is useful for understanding the rationale behind the choice.

1.6 Open raceway ponds

Main characteristics of open raceways are that the systems are open and microalgal cultures are directly exposed to the atmosphere (Malavasi et al.,2020). These are open channels that use a paddle-wheel mixer, which circulates the algae and nutrients. Variations of light and temperature are the most important climate factors affecting biomass productivity in outdoor cultivation; light is only perceived from the top layer of the pond, when light penetrates through the top, middle and bottom layers, the light intensity decreases due to absorption by the algae cells when light passes through the layers. For this, depth in raceways should have an optimal 30 cm to allow sunlight penetration. Since the system depends on sunlight as a source of energy, it is predominantly used for the production of large-scale microalgae, like *Chlorella* spp, *Dunaniella salina* and *Spirulina platensis.* The latter an extremophile species (Barboza- Rodriguez, R et al., 2024). The main advantages of open raceways ponds are low costs and ease of maintenance. Operating costs can be kept low by using only sunlight as primary energy input and the energy needed to mix the crops is relatively low (Colta 2023).

However, they have some disadvantages such as lower cell concentrations than other cultivation systems used, thus requiring an efficient harvesting method. Open ponds are at risk of several algal predators such as birds, frogs, aquatic insects, and a range of microorganisms might cause contamination of culture, and loss of biomass (Malavasi et al., 2020). In addition, issues like rainwater affect culture media by diluting, altering the

salinity and pH, and affecting biomass productivity (Barboza-Rodrìguez, R et al., 2024).

1.7 Photobioreactors (PBR)

The term photobioreactor refers to closed systems, sealed, illuminated, closed culture vessels locked with no gas exchange or contaminants. They are typically constituted of a four-phased system: microalgal (solid phase), culture media (liquid phase), O_2 or CO_2 (gaseous phase), and superimposed light-radiation field (Barboza-Rodrìguez, R et al., 2024).Compared to open ponds, PBRs facilitate better control of the growing environment and offer better control of conditions such as pH, temperature and light intensity. Reduce carbon dioxide loss, prevent water evaporation and can achieve much higher photosynthetic efficiency, productivity and biomass concentration The efficiency of PBRs is determined by the efficiency of luminous energy capture and transport, its distribution and the use of light by microalgae through photosynthesis (Colta et al., 2023). Biomass conversion efficiency is therefore seminal to increase the productivity of algae industrial cultivation and make it economically and energetically sustainable (Perin et al., 2017). PBR should ensure uniform illumination of the growing area (Colta et al., 2023). However, one of the drawbacks of growing algae in photobioreactors is inhomogeneous distribution of light in the culture due to cells selfshading. cells exposed to full sunlight easily experience saturating irradiation. (Perin et al.,2017). For this experiment, the photobioreactor (PBR) located in the laboratory of the A. Vallisneri Interdepartmental Complex was used (Fig. 6).

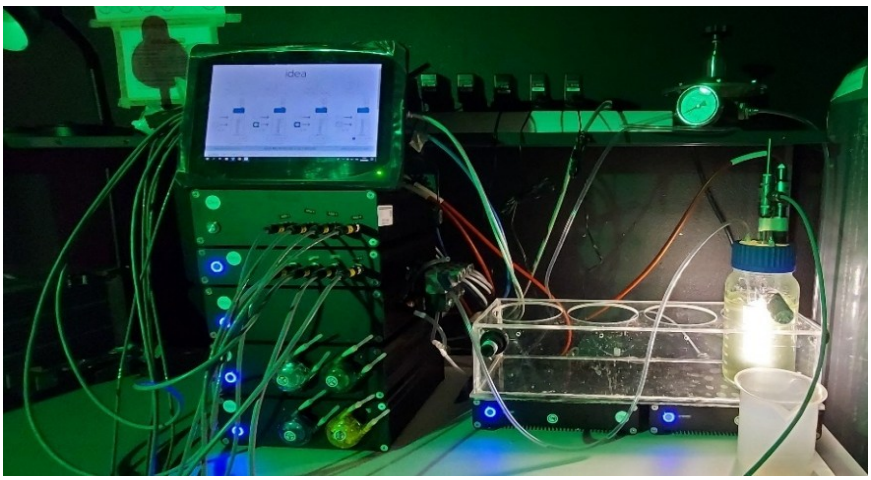

Fig. 6: Photobioreactor located in the A. Vallisneri Interdisciplinary Complex.

Open Raceway Ponds	Photobioreactors (PBR)
↑ Low installation and maintenance costs	↓ High installation and maintenance costs
↓ Higher risk of contamination	↑ Lower risk of contamination
↑ Easy operation and management	↓ Complex management and maintenance
↓ Environmental variability (light, temperature, rain)	↑ Better control over pH, temperature, and light
↑ Use of sunlight as an energy source	↓ Challenges in ensuring uniform illumination
↓ Lower cell concentration compared to PBRs	↑ Higher productivity and biomass concentration
↑ Suitable for large-scale production	↓ Possible self-shading of cells
↓ Lower photosynthetic efficiency	↑ Higher photosynthetic efficiency
	↑ Reduced water evaporation and CO2 loss

Table 1: Comparison between Open Raceway Ponds and PBR.

↑ indicates advantages
↓ indicates disadvantages

2 THESIS OBJECTIVES

This study aimed to investigate the physiological responses of desert microalgae cultivated under controlled conditions in a photobioreactor, in order to evaluate their potential for biotechnological applications.

The research was structured around the following hypotheses:

Hypotesis 1: Among desert soil microalgae, certain taxa (e.g. *Chlorella* spp.) exhibit greater resilience to environmental stresses (light intensity, pH, nutrient limitation, temperature) than others, allowing them to dominate under industrial cultivation conditions.

Hypotesis 2: Stress conditions in the photobioreactor induce measurable physiological responses in microalgae, reflected in growth dynamics (OD), pigment composition (chlorophyll a, chlorophyll b and carotenoids), and culture stability.

Hypotesis 3: Industrial cultivation parameters (e.g. semi-continuous dilutions, enriched media, photoperiod changes) significantly affect the balance between biomass accumulation and pigment production, highlighting trade-offs relevant for large-scale production.

Hypothesis 4: Molecular analysis through DNA extraction and metabarcoding sequencing will confirm whether the observed dominance of specific taxa is linked to their ability to withstand long-term cultivation under extreme stressors.

From a scientific perspective, the study highlights the adaptive potential of extremotolerant microalgae and their suitability as models for understanding resilience in arid ecosystems. From an applied perspective, it provides insights into the challenges and opportunities of cultivating desert microalgae at industrial scale.

Future research should:

- Confirm taxonomic identities via metabarcoding and link them to physiological traits.
- Optimize photobioreactor designs to reduce adhesion and improve light distribution.

- Explore metabolite production (e.g. carotenoids, antioxidants) under stress to assess industrial potential.

In conclusion, this work provides a critical step toward integrating desert microalgae into biotechnological applications, combining ecological relevance with economic opportunities in a climate change scenario.

3 MATERIAL E METHODS

3.1 BIODESERT

Soil samples were previously collected by BIODESERT, a research project funded by the European Research Council (Maestre 2017). It is a large cooperative field survey, which aims to establish a network of monitoring assessments between the arid areas of the globe, to assess how simultaneous changes in climate and grazing pressure affect both biotic factors, the multifunctionality of the ecosystem in global drylands. This survey is coordinated by Dr. Fernando T. Maestre of the Rey Juan Carlos University in Mòrtoles.

The project involves research groups from 27 countries: Argentina, Australia, Botswana, Brazil, Burkina Faso, Canada, Chile, China, Ecuador, Ghana, India, Iran, Israel, Kazakhstan, Kenya, Mexico, Mongolia, Morocco, Namibia, Niger, Peru, Portugal, South Africa, Spain, Tunisia, USA and Venezuela, covering 263 dryland ecosystems from all continents except Antarctica (Fig. 7). Data is shared in a centralized repository at URJC (Maestre 2017).

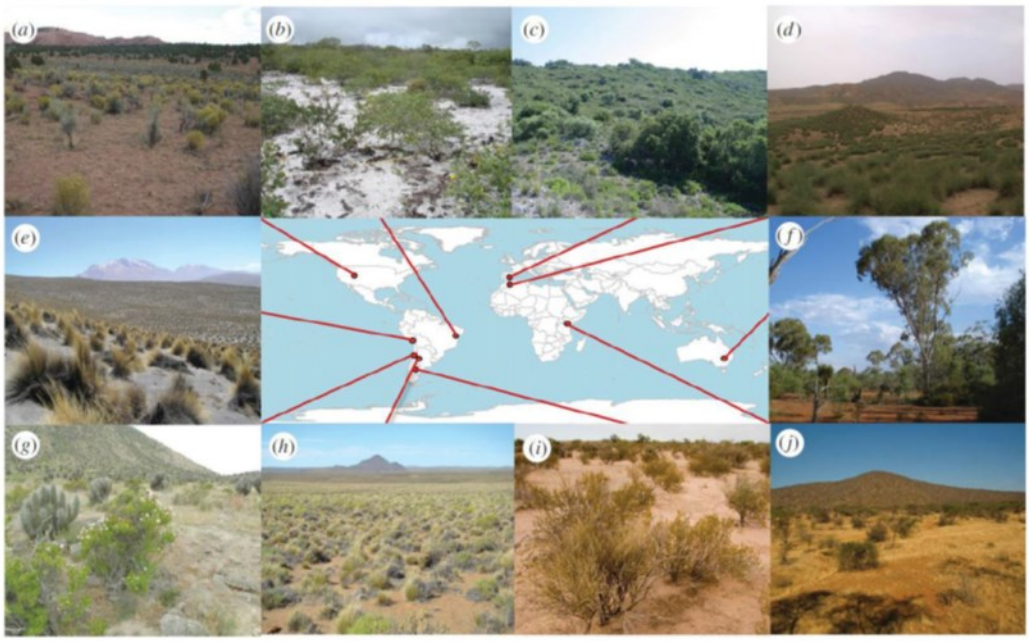

Fig. 7: Some drylands area surveyed across the world by the BIODESERT project.

3.2 Algae inoculum establishment

Soil samples from 14 different countries were considered (table 2), which were previously stored at a -20°C temperature.

Soil ID	Country	Site
FM 2	Algeria	El Ouassria
FM 8	Argentina	Pilcaniyeu
FM 37	Australia	Hay site
FM 52	Canada	Lac du Bois
FM 66	China	Muri
FM 90	Iran	Lohondor
FM 114	Israel	Sayeret Shaked
FM 122	Mexico	La Flor
FM 135	Mongolia	Shand
FM 173	Portugal	Castro Verde
FM 197	South Africa	Lichtenburg
FM 207	Spain	Ciempozuelos
FM 235	Tunisia	Guelb Fguira
FM 258	USA	IBP

Table 2: Sampling sites and countries of soil origin used for inoculum preparation.

3.3 BBM+C

The Bold's Basal Medium (BBM) (Bischoff & Bold, 1963) is a culture medium that can be used to grow various types of microalgae. The fungicide Carbendazim 97% (Aldrich), vitamins and Soil Extract were added to BBM, hence it is called BBM+C. For this experiment, BBM+C soil without agar was prepared.

#	Component	Final concentration	Stock solution ($g \cdot L^{-1}$ dH_2O)	Addition per 1 Litre culture medium
1	$NaNO_3$	2.94 mM	25.00	10 ml
2	$CaCl_2 \cdot 2H_2O$	0.17 mM	2.50	10 ml
3	$MgSO_4 \cdot 7H_2O$	0.3 mM	7.50	10 ml
4	K_2HPO_4	0.43 mM	7.50	10 ml
5	KH_2PO_4	1.29 mM	17.50	10 ml
6	NaCl	0.43 mM	2.50	10 ml
7	Alkaline EDTA solution EDTA (Titriplex III) KOH	 17.10 mM 55.30 mM	 50 g 31 g	1 ml
8	Acidified Iron solution $FeSO_4$ x 7 H_2O H_2SO_4	 0.179 mM	 4.98	1ml
9	Boron solution H_3BO_3	 18.50 mM	 11.42	1ml
10	Trace Metals solution $ZnSO_4$ $7H_2O$ $MnCl_2$ $4H_2O$ MoO_3 $CuSO_4$ $5H_2O$ $Co(NO_3)_2$ $6H_2O$	 8.82 1.44 0.71 1.57 0.49	 0.307 µM 7.28 µM 4.93 µM 6.29 µM 1.68 µM	1ml

Table 3: composition of culture medium BBM+C.

For the preparation of a BBM+C batch, 500mL of ultrapure water was poured in a bottle with a magnet inside, the bottle was placed on a magnetic stirrer (under slight agitation without heating), subsequently 1mL of Carbendazim was added and 20mL of BBM Sigma, previously chilled at 4°C. The fungicide was kept in agitation during withdrawal, covered with parafilm. Finally, 10 mL of Soil Extract were thawed at room temperature and then added to the medium. Pure water was then added up to a final volume of 1000 mL.

The magnet was then removed, and the growth medium was autoclaved.

Following autoclaving, the medium was allowed to cool to room temperature, after which 1 mL of the vitamin solution was added.

COMPONENT	PRODUCT	CONCENTRATION FOR 1L
Fungicide	Carbendazim	1mL/L
Soil Extract		10mL/L
Bold Basal Medium	BBM Sigma	20mL/L
Vitamins	Vitamix 1000	1mL/L

Table 4: Composition of culture medium BBM+C.

3.4 First photobioreactor experiment

The inoculum had already been prepared by others, containing a total of 100 mL of solution composed of BBM+C medium and all the soils listed in Table 2. After preparation, it was kept in a growth chamber under 24h photoperiod (24 hours of light) and a constant temperature of 22°C to promote and accelerate biomass growth.

After 38 days, it was brought to the laboratory located at the A. Vallisneri Interdisciplinary Department for the preparation of the photobioreactor experiment.

Into the 1000 mL photobioreactor bottle were added: 900 mL of BBM+C and 100 mL of inoculum.

Fig. 8: 18/01/2024. First day of the photobioreactor experiment.

3.5 Growth monitoring

The growth and fitness of the microalgae were monitored using a visible light spectrophotometer. Throughout the experiment, growth was monitored at 710 nm (wavelength), which is typically used to track the growth of algae and microalgae.

Initially, monitoring was carried out every 2–3 days, as growth is slow during the early stages, and the measurement frequency was then increased as the growth rate accelerated.

3.6 Sample dilution

Due to the continuous aggregation of biomass on the walls of the bottle, 300 mL were removed from the sample and replaced with 300 mL of fresh BBM+C medium.

With the addition of fresh medium, hence increasing the batch nutrients and diluting the cell concentration, and improvement on the situation was expected. However, the situation remained unchanged, so another strategy was researched.

For reasons reported in section 4.1, it was necessary, after just under two months of work, to remove the culture from the photobioreactor.

3.7 Second photobioreactor experiment

The soils in Table 2 have been taken up

An equal amount of each sample was placed in Petri dish to allow them to dry for at least one night at room temperature (Fig. 9).

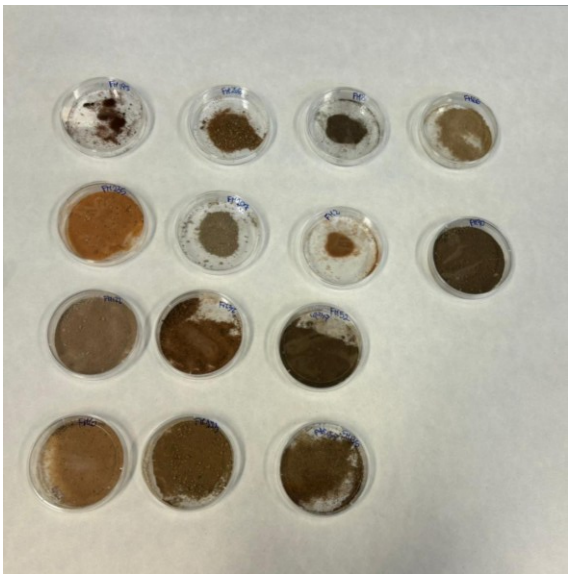

Fig. 9: The 14 soil samples cryo-conserved.

3.8 Culture establishment with samples of soil

1,5 g (2 mL) of each soil sample and 50 mL of autoclaved water were taken and transferred into a conical flask, which was placed in agitation for 10 minutes. Each flask contained a different soil sample. (Fig. 10).

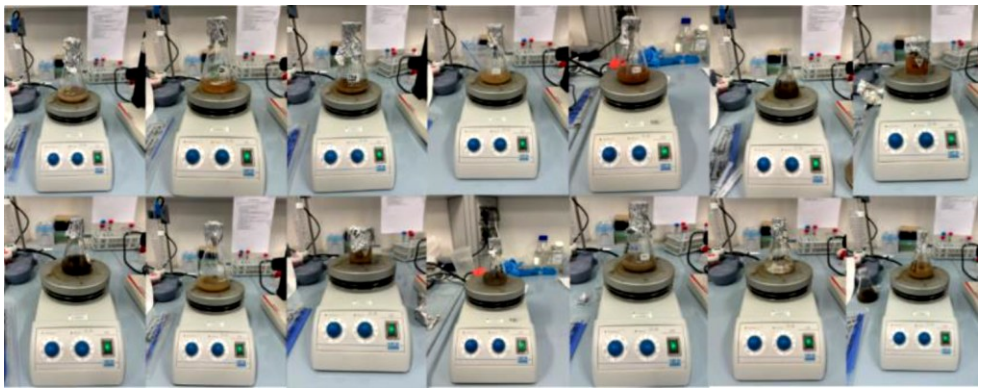

Fig. 10: Agitation of the 14 soil samples.

3.9 Inoculum establishment with samples of soil

In a 1L flask, 500 mL of BBM+C medium were inserted, and then positioned on top of a magnetic stirrer with active agitation.

At time = 0, 50 uL of the first sample were added to the medium. After 10 minutes, 50 uL of the second sample were added to the same flask.

This procedure was then replicated every 10 minutes for the rest of the samples.

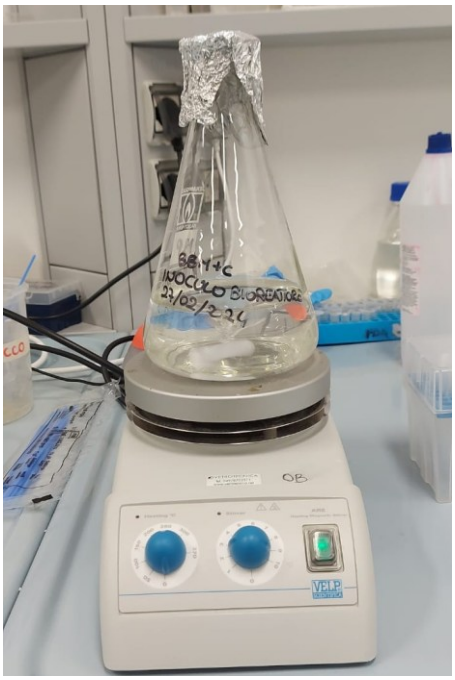

Fig. 11: Agitation of the inoculum.

At the end of the addition process, the inoculum was placed in the growth chamber under the same growth conditions as the first experiment.

The experiment in the PBR began 14 days after the inoculum was prepared, thus earlier compared to the first experiment (Fig. 12).

Fig. 12: Sample just inoculated (left), and 14 days later (right).

3.10 Growth monitoring

The second PBR experiment was carried out like descibed before (section 3.4). However, instead of measuring the absorbance values with different frequency depending on growth, this time these (750 nm) were periodically measured (Fig. 13). This measurement mainly reflects the turbidity of the sample, proportional to the concentration of cells in suspension, far from the absorbance region of pigments (chlorofillae and carotenoids), which absorb particularly between 400–700 nm.

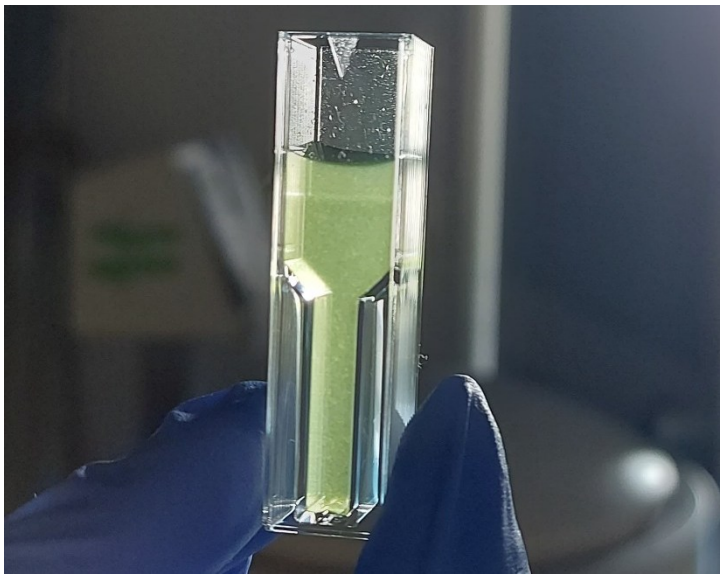

Fig. 13: Cuvette containing culture sample diluted 1:1 with deionized water.

Two cuvettes were prepared for each absorbance value, allowing for two measurements to be taken. If one of the two values was significantly different, a third cuvette was prepared, and a third measurement was taken.

Throughout the entire duration of the work, an effort was made to remain within the value of 1 g/L, which represents the standard condition used to simulate an industrial growth environment.

3.11 Sample dilution and introduction of water bath

To promote an increase in nutrients, 600 mL of culture were removed and replaced with 600 mL of fresh BBM+C medium. Additionally, a water bath was introduced to maintain a constant temperature and prevent the culture from overheating.

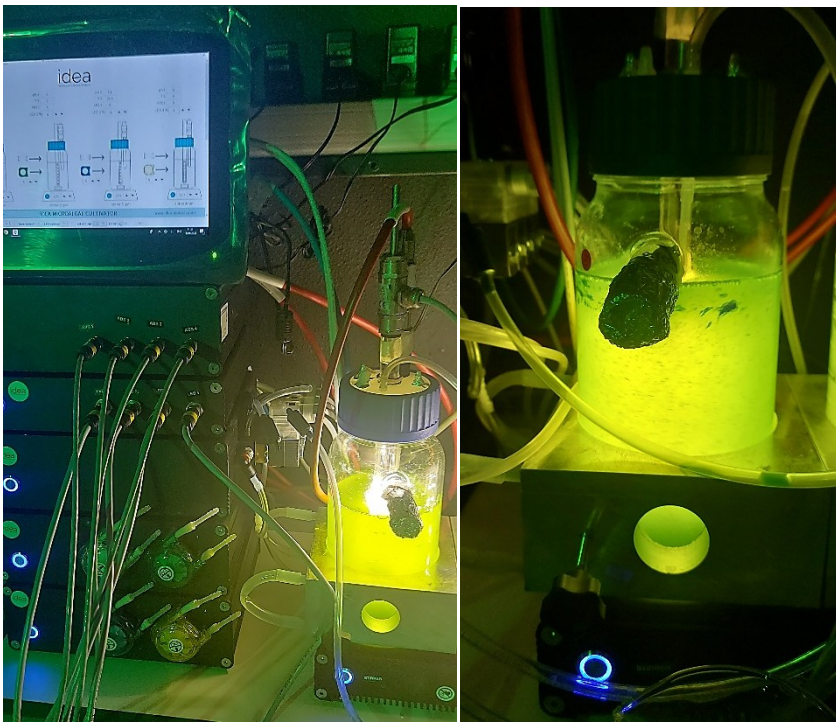

Fig. 14: Photobioreactor in Vallisneri's lab with water bath.

3.12 Nutrient enrichment of the medium

As the expected increase in growth was not achieved with the previous dilution, it was decided to increase the concentration of nutrients ($NaNO_3$, K_2HPO_4, and KH_2PO_4) in fresh medium (a bottle containing 400 mL of fresh BBM+C was used) and subsequently perform a dilution.

In 400 mL of growth medium were added:

- 50mL di $NaNO_3$ 25 g/L
- 25mL di K_2HPO_4 7,50 g/L
- 25mL di KH_2PO_4 17,5 g/L

Final concentration $NaNO_3$

Mass added : 25,00 $g*L^{-1}$ * 0,050 L = 1,250 g

Final concentration : 1,250 g / 0,4 L = 3,125 g/L

Final concentration K_2HPO_4

Mass added : 7,50 $g*L^{-1}$ * 0,025 L = 0,1875 g

Final concentration : 0,1875 g / 0,4 L = 0,46875 g/L ≈ 0,469 g/L

Final concentration KH_2PO_4

Mass added : 17,50 $g*L^{-1}$ * 0,025 L = 0,4375 g

Final concentration : 0,4375 g / 0,4 L = 1,09375 g/L ≈ 1,094 g/L

Nutrients	Stock (g/L)	Volume added (L)	Mass added (g)	Final concentration (g/L)
$NaNO_3$	25,00	0,050	1,250	3,125
K_2HPO_4	7,50	0,025	0,1875	0,469
KH_2PO_4	17,50	0,025	0,4375	1,094

Table 5: Summary of the nutrient concentrations in the enriched BBM+C medium (400 mL).

Subsequently, a dilution was performed by adding 400 mL of nutrient-enriched medium to the culture. At the same time, the same volume was removed to maintain a constant total volume.

3.13 Preparation of stock solutions of $NaNO_3$, KH_2PO_4, K_2HPO_4

Despite the enrichment of the BBM+C medium as reported in Table 5, microalgal growth remained limited.

To verify whether this limitation was due to nutrient scarcity, an enhanced medium was prepared with increased concentrations ($NaNO_3$ 50X, KH_2PO_4 200X, and K_2HPO_4 200X).

To improve efficiency and precision in the work, stock solutions of the nutrients listed in Table 5 were prepared, to be subsequently used for different dilutions, thereby avoiding repeated preparations.

$NaNO_3$

As shown in Table 3, the $NaNO_3$ stock solution is $25\frac{g}{L}$. The required amount of NaNO3 was calculated to obtain 500mL of 50X stock solution (50 times more concentrated than the final concentration, namely $10\frac{g}{L}$).

The prepared stock volume was 500mL, containing 250g of $NaNO_3$, with a resulting concentration of $500\frac{g}{L}$.

Based on the stock solution concentration, the desired final concentration of the salt in the medium was determined, keeping the final culture volume unvaried.

C1 * V1 = C2 * V2

C2 = ($500\frac{g}{L}$ / 50) = $10\frac{g}{L}$.

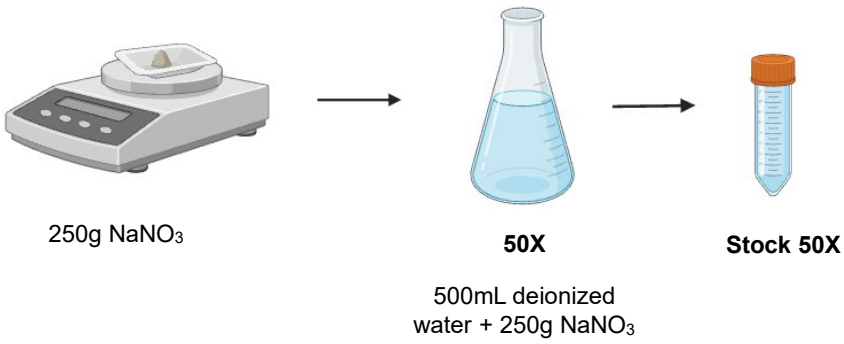

Fig. 15: Workflow for stock preparation.

Subsequently, the volume of stock solution to be taken from the Falcon tube and added to the fresh BBM+C medium was determined.

C1 * V1 = C2 * V2

V1 = $(10\frac{g}{L}$ * 1L) / $500\frac{g}{L}$

V1= 0,02 L → <u>20mL</u>

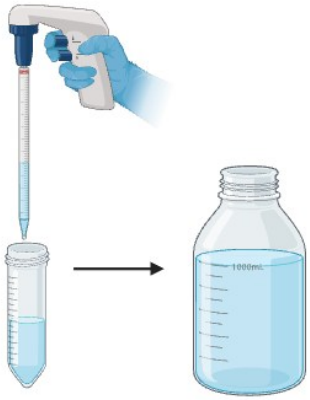

Fig. 16: Final step: withdrawal of the stock and inoculation into fresh BBM+C medium.

KH_2PO_4

According to Table 3, the standard final concentration of KH_2PO_4 in the BBM+C medium is $0{,}175\ \frac{g}{L}$.

To obtain a final 5X concentration, the value was multiplied by 5, resulting:

$0{,}175\frac{g}{L}$ * 5 = $0{,}875\ \frac{\mathrm{g}}{\mathrm{L}}$

For the preparation of 100 mL of a 200X stock solution, the mass of KH_2PO_4 to be weighed was calculated:

mass= $0{,}875\ \frac{g}{L}$ * 0,1 L * 200 = <u>17,5g</u>

Considering the weighed mass and the prepared volume, the concentration of the 200X stock solution is $175\ \frac{g}{L}$.

Subsequently, the solution was divided into two 50mL Falcon tubes, while maintaining the concentration unchanged.

The prepared stock for the experiment was therefore 200 times more concentrated than this hypothetical value.

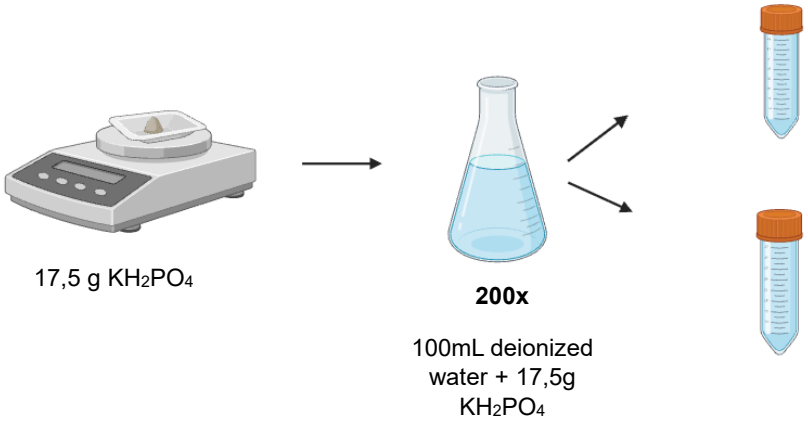

Fig. 17: Workflow for stock preparation.

Finally, the volume of the stock solution to be taken from the Falcon tube and added to obtain 1000 mL of enhanced BBM+C medium was determined.

C1 * V1 = C2 * V2

V1 = (0,875 $\frac{g}{L}$* 1L) / 175 $\frac{g}{L}$

V1= 0,005 L → <u>5mL</u>

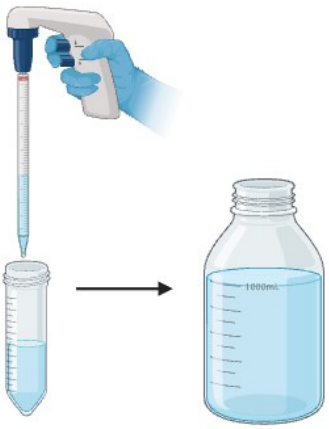

Fig. 18: Final step: withdrawal of the stock and inoculation into fresh BBM+C medium.

K_2HPO_4

A 200X stock solution was prepared (Table 3).

Final concentration standard medium = 7,5 $\frac{g}{L}$ * 0,010 L * $\frac{1}{L}$= 0,075 $\frac{g}{L}$.

Final concentration enhanced medium= 0,075 $\frac{g}{L}$ * 5 = 0,375 $\frac{g}{L}$.

As done previously, 100 mL of a 200X stock solution were prepared, calculating the mass of K_2HPO_4 to be weighed:

mass = 0,375 $\frac{g}{L}$ * 0,1 L * 200 = <u>7,5 g</u>

The concentration of the 200X stock solution was therefore 75 $\frac{g}{L}$.

The prepared solution was then transferred into two 50 mL Falcon tubes.

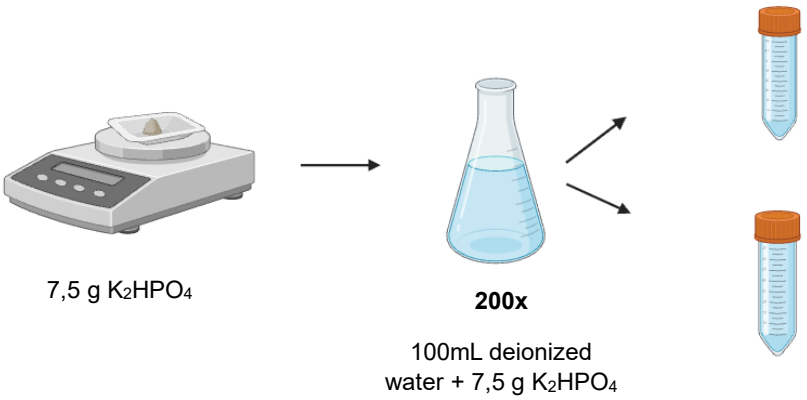

Fig. 19: Workflow for stock preparation.

Finally, the volume of the stock solution to be used for 1000mL of medium was determined.

C1 * V1 = C2 * V2

V1= (0,375 $\frac{g}{L}$ * 1L) / 75 $\frac{g}{L}$

V1 = 0,005 L → <u>5mL</u>

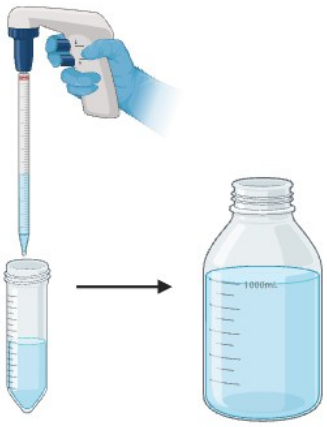

Fig. 20: Final step: withdrawal of the stock and inoculation into fresh BBM+C medium.

Composto	Conc. stock standard (g/L)	Conc. finale nel terreno (g/L)	Conc. stock preparata (g/L)	Massa pesata (g)	Volume preparato (L)
$NaNO_3$	25,0	0,250	500	250	0,50
KH_2PO_4	17,5	0,175	175	17,5	0,10
K_2HPO_4	7,5	0,075	75	7,5	0,10

Table 6: Calculated values for the preparation of stock solutions of $NaNO_3$, KH_2PO_4, and K_2HPO_4 used in BBM+C medium.

3.14 Semicontinuous dilutions and biomass calculation

In order to maintain the cells in exponential growth and to subsequently recover biomass, semicontinuous dilutions were carried out on alternate days.

3.14.1 Semicontinuous dilutions

After preparing the nutrient stock solutions, 1 L of fresh BBM+C medium was enriched, as reported in Table 6 the following were added:

$NaNO_3$: 20mL

KH_2PO_4: 5mL

K_2HPO_4: 5mL

The amount of material removed during the dilutions was not the result of specific calculations but varied according to the growth trend of the microalgae.

3.14.2 Calculation of biomass before and after dilution

Before and after each dilution, samples were taken from the photobioreactor for spectrophotometer analysis, as performed daily, and subsequently filtered to calculate the amount of biomass present.

Before starting each filtration, the filter paper was placed in an oven for four hours to dry it from residual moisture and subsequently weighed.

The sample taken from the PBR was placed in a beaker, from which 5 mL were withdrawn and transferred into a 50 mL Falcon tube with the addition of 15 mL of deionized H_2O.

- Falcon tube before dilution: 5 mL of sample, with the addition of 15 mL of deionized H_2O.

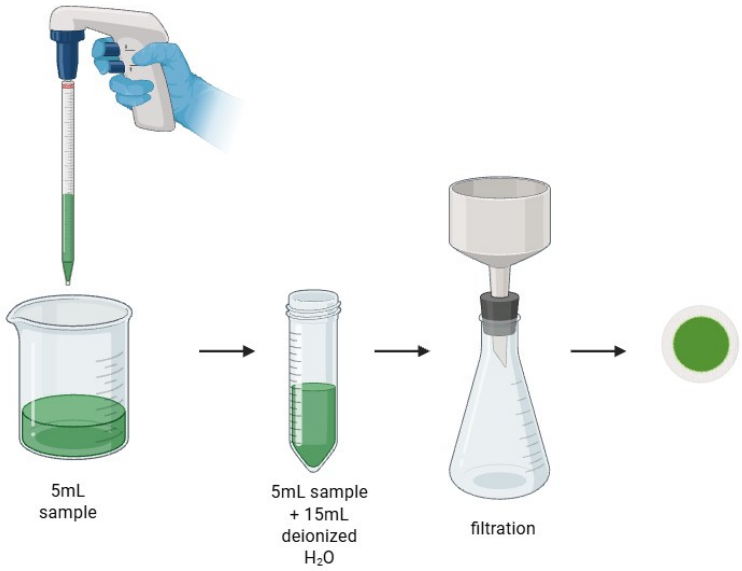

Fig. 21: Filtration workflow for biomass recovery prior to dilution.

- Falcon tube after dilution: 5 mL of sample, with the addition of 15 mL of deionized H_2O.

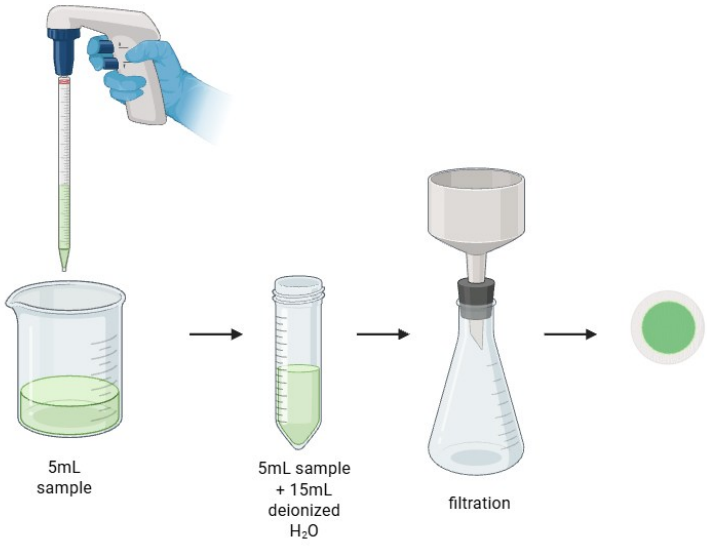

Fig. 22: Filtration workflow for biomass recovery after dilution.

Afterwards, the filters were placed in an oven and weighed the following day to calculate the amount of biomass present using the following formula:

$$\text{Biomass}_{\text{dry}} = \frac{m_{filter+biomass} - m_{filter}}{V_{culture}}$$

- $m_{filter+biomass}$ = mass of the filter after filtration and drying in the oven.
- m_{filter} = mass of the dry filter before filtration.
- $V_{culture}$ = volume of the filtered sample.

This procedure was carried out for every semicontinuous dilution.

3.15 Photoperiod setup

A 16 hours photoperiod (16 h of light and 8 hours of dark) was applied for a duration of three months. The main objective was to promote faster growth of the culture. In addition to the photoperiod, the LED intensity was reduced from 100% (3000 µmol/m²·s) to 43% (1290 µmol/m²·s) to observe the growth curve as the LED intensity gradually increased back to 100%.

Following this step, semicontinuous dilutions were performed very other day, with subsequent sampling and monitoring of biomass quantity.

The LED intensity was raised to 100% only in the final phase of the experiment because of the decrease in culture growth.

3.16 Preparation of samples for absorbance measurement

On the 136th day of the experiment, samples were prepared for monitoring the absorbance curve.

a) Two milliliters were collected and placed into two reaction microtubes:
- Microtube 1: 2 mL of material collected before dilution.
- Microtube 2: 2 mL of material collected after dilution.

b) The microtubes containing the material were centrifuged at 5000 rpm for 7 minutes. Subsequently, the surnattant was remuved and 1.5 mL of sample was added to each tube, followed by a second centrifugation at 5000 rpm for 7 minutes.

This procedure resulted in the collection of the pellet only.

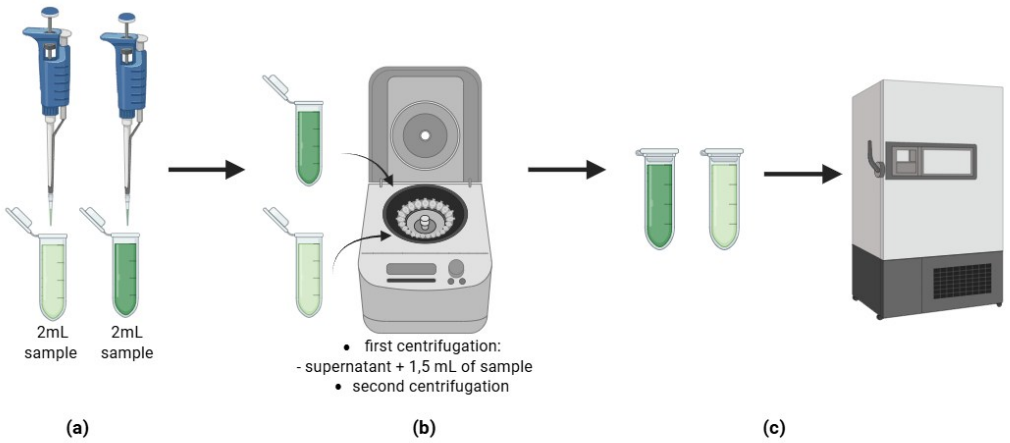

Fig. 23: Workflow for the preparation of samples for absorbance measurement.

c) The tubes were then sealed and stored at -20°C.

3.17 Sample preparation for DNA extraction

On the same working day as the preparation of samples for the absorbance curve, samples were prepared for DNA extraction. The extraction was carried out two months after the start of sample collection.

a) 1 mL of sample was collected before dilution and 1 mL after dilution, and added to two separate 2 mL screw-cap cryogenic tubes.
b) The tubes were then centrifuged at 5000 rpm for 7 minutes.
c) Subsequently, the supernatant was removed, and 1 mL of sample was added to each tube.
d) Another centrifugation was performed at 7000 rpm for 7 minutes. This way, each tube contained the pellet resulting from 2 mL of sample.

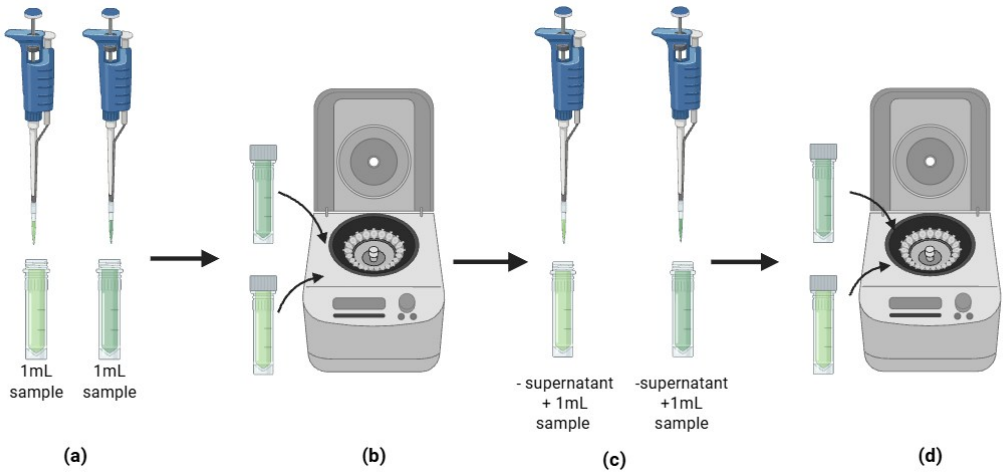

Fig. 24: Workflow for the preparation of samples for DNA extraction.

Finally, the tubes were immersed in liquid nitrogen, labeled, and stored in a -80°C freezer.

Both of these steps were performed after each semicontinuous dilution, following the 136th day of the experiment.

3.18 Absorbance curve measurement

On the 158th day from the start of the experiment, previously prepared samples (Section 3.16) were used to perform the absorbance curve in order to monitor the growth of the microalgae. This approach was applied not only to estimate the amount of biomass present, but more importantly to determine the photosynthetic pigment content in the analyzed samples. Such information provides an indication of the metabolic “activity” of the culture.

The blank used was DMF (N,N-dimethylformamide), a polar organic solvent capable of penetrating the membrane and solubilizing pigments (chlorophyll a, chlorophyll b, and carotenoids). This way, the pigments are released into the solvent and can be measured without interference from the cellular structure. Each sample was diluted, with the dilution factor adjusted according to the amount of material present.

Sample label	Dilution	Sample volume (µL)	DMF volume (µL)	Final volume
29/07/2024 sample 1	1:7	30µL	200µL	230µL
29/07/2024 sample 2	1:7	30µL	200µL	230µL
31/07/2024 sample 1	1:5	50µL	200µL	250µL
31/07/2024 sample 2	1:5	50µL	200µL	250µL
2/08/2024 sample 1	1:5	50µL	200µL	250µL
2/08/2024 sample 2	1:5	50µL	200µL	250µL
5/08/2024 sample 1	1:5	50µL	200µL	250µL
5/08/2024 sample 2	1:5	50µL	200µL	250µL
7/08/2024 sample 1	1:7	30µL	200µL	230µL
7/08/2024 sample 2	1:7	30µL	200µL	230µL
9/08/2024 sample 1	1:7	30µL	200µL	230µL
9/08/2024 sample 2	1:7	30µL	200µL	230µL

Table 7: Table summarizing the sample dilutions performed for absorbance curve measurements.

The formulas reported by (Wellburn 1994) were used to calculate the concentration of pigments (chlorophyll a, chlorophyll b and carotenoids) from the measured absorbance values:

- **Chl a** = $12.00 \times A_{663.8} - 3.11 \times A_{646.8}$
- **Chl b** = $20.78 \times A_{646.8} - 4.88 \times A_{663.8}$
- **Chl + C** = $(1000 \times A_{480} - 1.12 \times \text{Chl a} - 34.07 \times \text{Chl b}) / 245$

Table 12 reporting all pigment concentration calculations, obtained using the formulas cited above, is provided in the Appendix.

Concentration values were normalized to the optical density at 750nm, used as a proxy for biomass, in order to enable comparison among samples with different biomass amounts.

3.19 DNA extraction

The final step of the study took place on the 186th day from the start of the experiment, with the application of metabarcoding techniques to determine the species composition within the photobioreactor sample.

This molecular analysis technique involves DNA extraction from selected samples, amplification of one or more marker regions, and high-throughput sequencing to identify the organisms present.

Samples collected in the previous weeks (Section 3.17) were used. DNA extraction was performed with the Quick-DNA™ Fecal/Soil Microbe Microprep Kit, specifically designed for fecal and soil samples (≤ 250 mg), as in this experiment.

Procedure for DNA Extraction of Each Sample:

1- Soil samples were added to a ZR BashingBead™ Lysis Tube (0,1 & 0,5 mm). 750µL BashingBead™ Buffer were added to the tube.
2- The tubes were placed in a bead beater.
3- The ZR BashingBead™Lysis Tube (0,1 & 0,5 mm) was centrifuged in a microcentrifuge at 10,000 x g for 1 minutes.
4- 400µL supernatant was transfered to a Zymo-Spin™ III-F Filter in a Collection Tube and it was centrifuged at 8,000 x g for 1 minute. Zymo-Spin™ III-F was discarded.
5- 1,200µL of Genomic Lysis Buffer was added to the filtrate in the Collection Tube from Step 4. It was mixed well.
6- 800µL of mixture from Step 5 was transfered to a Zymo-Spin™ IC Column[3] in a Collection Tube and was centrifuged at 10,000 x g for 1 minute.
7- The flow through was discarded from the Collection Tube and the Step 6 was repeated.

8- 200µL DNA Pre-Wash Buffer was added to the Zymo – Spin™ IC Column in the NEW Collection Tube and it was centrifuged at 10,000 x g for 1 minute.
9- 500µL g-DNA Wash Buffer was added to the Zymo-Spin™ IC Column and it was centrifuged at 10,000 x g for 1 minute.
10- Zymo-Spin™ IC Column was transfered to a clean 1,5mL microcentrifuge tube and 20µL DNA Elution Buffer was added directly to the column matrix. It was centrifuged at 10,000 x g for 30 seconds to elute the DNA.
11- Zymo-Spin™ II - µHRC Filter was placed in a clean Collection Tube and 600µL Prep Solution was added. It was centrifuged at 8,000 x g for 3 minutes.
12- The eluted DNA was transfered to a prepared Zymo-Spin™ II-µHRC Filter in a cleann 1,5 mL microcentrifuge tube and it was centrifuged at exactly 16,000 x g for 3 minutes.

Finally, the samples were submitted to Novogene for metabarcoding analysis.

4 RESULTS AND DISCUSSION

4.1 Growth dynamics under stress conditions

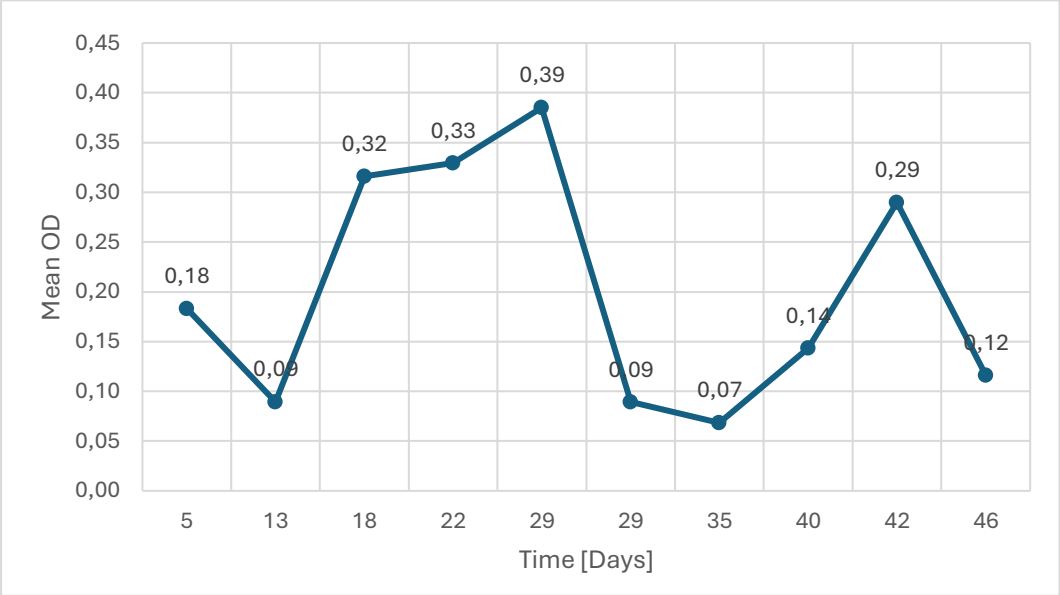

Fig. 25: Graph showing the progression of culture growth in the first experiment across daily measurements.

Both experiments demonstrated that desert microalgae can survive for several months in photobioreactor (PBR) conditions, even when exposed to multiple stressors. The values reported for the first experiment correspond to optical density (OD) measurements at 710 nm. For each time point, two measurements of the same sample were collected, and when necessary a third replicate was added. Growth trends were then analyzed in relation to monitoring days.

Subsequently, pH values, LED intensity, and temperature were also monitored. Initially, the LED intensity was kept low to avoid excessive stress on the culture and to promote growth. Temperature was likewise monitored, maintaining low values at first, then gradually increased.

After a few days, however, the culture exhibited uneven growth, with most biomass adhering to the LED and the pH meter rather than being evenly distributed in the medium. For the purpose of this study, cells needed to remain in suspension.

It is important that microalgae within a closed PDB system remain in suspension for several reasons:

1. Uniform access to light

The growth of microalgae depends on photosynthesis. When the cells remain in suspension, each cell receives, on average, a more uniform amount of light, thereby avoiding shaded zones and localized photoinhibition. If they adhere to the walls, only those directly exposed to light can continue growing, while the few cells left in suspension experience reduced light transmission.

2. Better nutrient and gas exchange

Microalgae in suspension have better access to nutrients and dissolved CO_2, as well as a more efficient way to eliminate excess O_2. In contrast, attached microalgae (biofilms) may face limitations due to restricted nutrient and gas diffusion through the cell layer.

3. Higher Photobioreactor Efficiency

The adhesion of biomass to the internal surfaces fouls and clouds the photobioreactor, making continuous cleaning operations necessary. The resulting reduced light penetration lowers photosynthetic efficiency and increases both additional costs and labor time.

4. Easier minitoring and control of culture parameters

In suspension, biomass density can be more easily monitored, and parameters such as pH, LED light intensity, nutrient concentration, and temperature can be controlled regularly and precisely. Without suspension, the system becomes less homogeneous, and even biomass harvesting becomes more complex.

Considering these aspects, on day 29, replacement dilution was performed (adding 300 mL of fresh medium) to clean the culture and increase the nutrient concentration. Despite this intervention, algae remained attached to the immersed instruments , hindering light penetration and resulting in very slow growth.

In the final days, pH, LED light intensity, and temperature were increased in hopes of recovery, but growth did not improve. Consequently, the first experiment was terminated and a new inoculum was prepared using the same soils.

This outcome can be explained by the fact that, prior to the start of the experiment, algal biomass had already accumulated for 38 days in the inoculum, leading to rapid adhesion to the LED and pH probe and compromising the study.

4.2 Culture observations

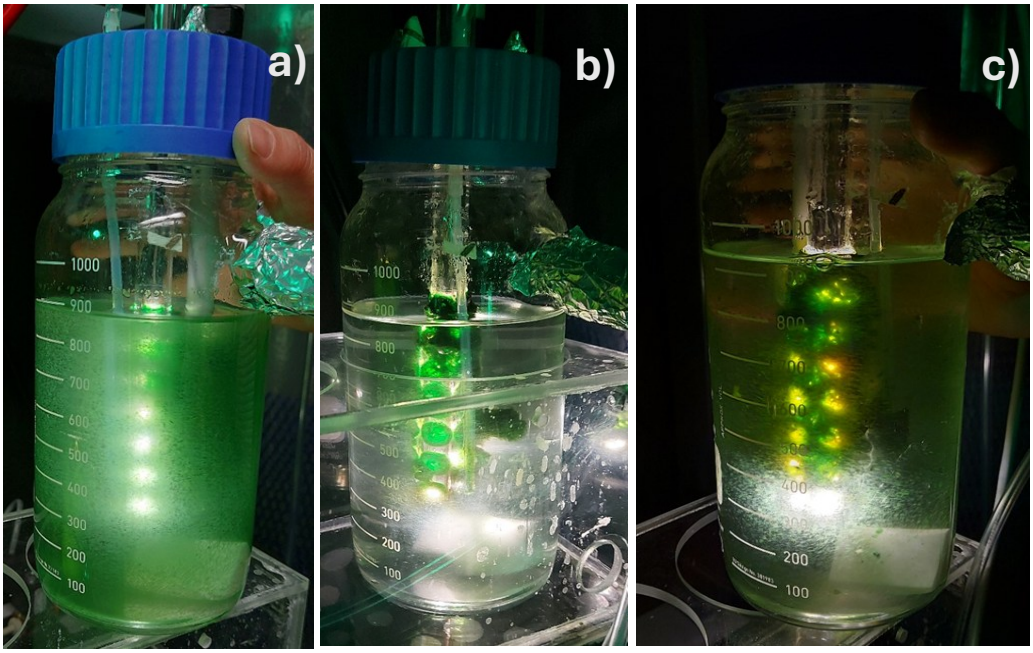

Fig. 26: a) First growth microalgae phase; b) second growth microalgae phase; c) third growth microalgae phase.

a) Photo taken on the 13th day of the experiment. For such an early stage, the amount of biomass was quite concentrated, and part of it was already adhering to the LED.
b) Photo taken on the 35th day, after the replacement dilution. The concentration of suspended algae in the medium had consequently decreased significantly; indeed, the medium appeared almost transparent. However, following the dilution, detachment of algae from the LED and pH meter was expected. Furthermore, growth in suspension was particularly slow, likely due to limited light penetration caused by algae aggregation on the LED.
c) Photo taken on the last day, shortly before terminating the experiment. Light penetration was very limited, as was the amount of suspended material. Carotenoids were observed, likely as a protective response to intense light.

4.3 Monitoring status of culture in the second experiment

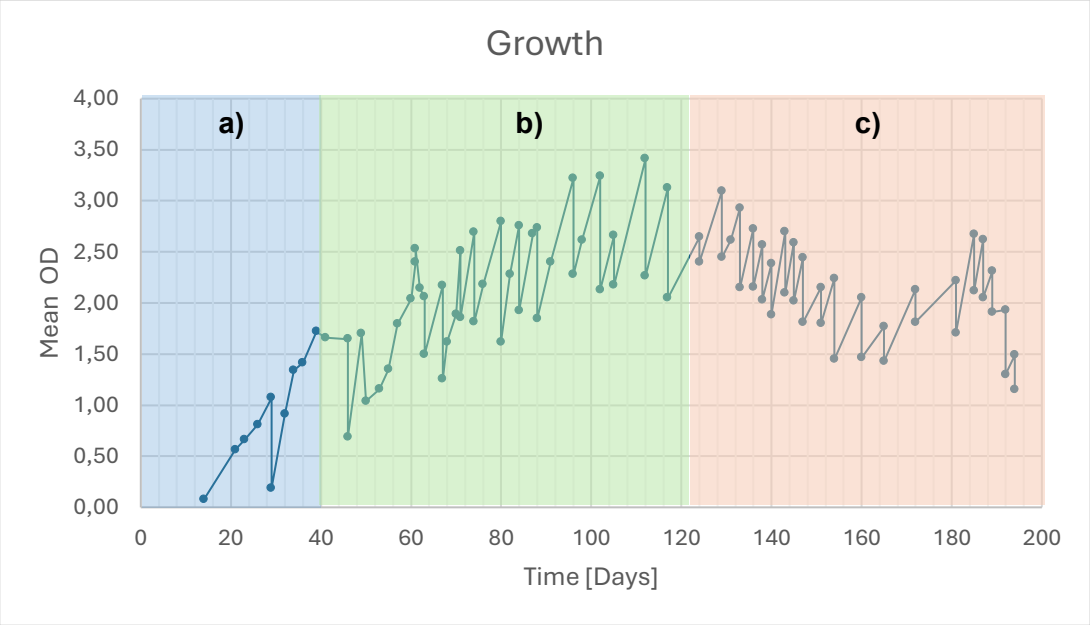

Fig. 27: Graph showing the progression of culture growth across daily measurements.

a) During the first phase (approximately 0–40 days), the culture showed a rapid increase in OD, indicating an exponential growth phase.

b) Growth stabilized (approximately 40–120 days). During this phase, semi-continuous dilutions were performed every other day to keep the culture within a controlled growth range. Significant fluctuations in OD values were observed. These variations are not only due to environmental stress factors (light intensity, nutrient availability, pH, and temperature) but are primarily caused by the semi-continuous dilutions, which were necessary to maintain the culture within a controlled growth range.

c) From around day 120, OD values showed a slight decreasing trend, although oscillations remained consistent. This may indicate a gradual decline in metabolic activity and biomass accumulation, potentially due to the introduction of the photoperiod on day 104, with 16 hours of light and 8 hours of darkness. This occurs because during the dark hours no photosynthesis takes place in the microalgae, while respiration continues, leading to the consumption of energy reserves. As a result, biomass accumulation is slowed down.

Overall, the general upward trend observed throughout the cultivation period indicates that the system maintained metabolic activity even under prolonged and high-stress conditions. However, the fluctuations and the final decline highlight the challenges in maintaining stable biomass productivity for desert microalgae under lab-scale cultivation conditions.

4.4 Culture observations

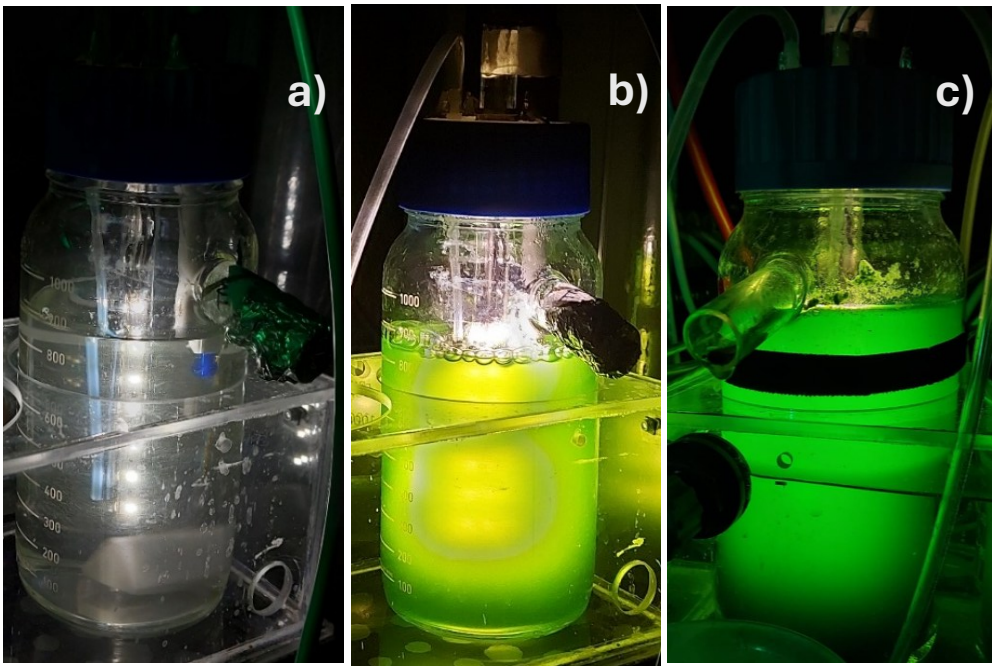

Fig. 28: a) First growth microalgae phase; b) second growth microalgae phase; c) third growth microalgae phase.

a) This photo, taken during the first days of the experiment, shows a lag phase, with minimal growth.
b) This image shows the biomass during the exponential growth phase, highlighted by the intense green color of the culture, indicating a high concentration of photosynthetic cells in suspension. The yellow-green observed is attributed to the accumulation of photosynthetic pigments (chlorophylls and carotenoids). This represents the period of maximum cellular productivity, with a significant increase in optical density and dry biomass.
c) Compared to the previous photo, the culture appears opaquer and more compact, indicating that chlorophyll and carotenoid levels have

reached high concentrations. The uniform color distribution across the liquid suggests that operational conditions ensured good cell suspension and effective light exposure. However, some aggregation along the container walls is observed, possibly indicating stress due to nutrient limitation or light intensity. In this phase the LED intensity was mainteined at 100%.

4.5 Microscopic observations

4.5.1 Intermediate phase of the experiment

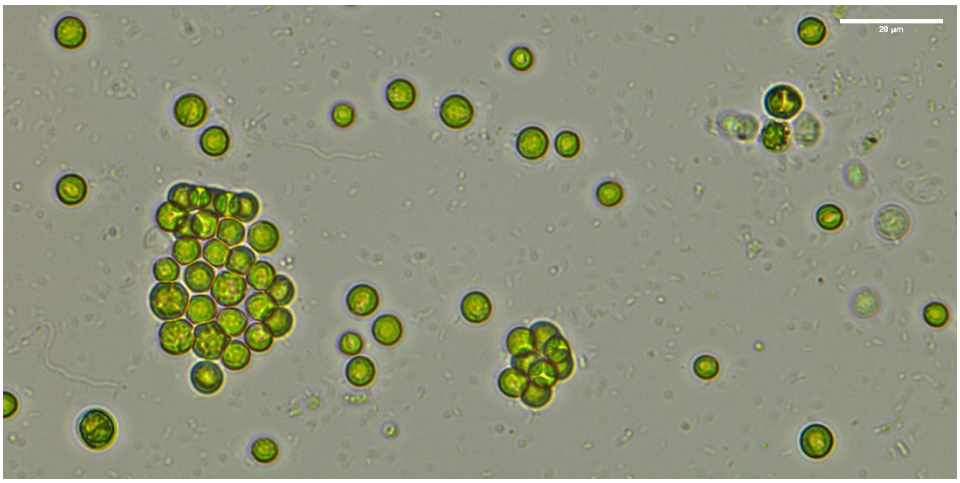

Fig. 29: Microscopic view (20x) of the culture at the intermediate phase of the experiment.

The slides were observed under the microscope during the intermediate phase of the experiment (approximately day 90), in which the culture was subjected to a 30°C, and a pH of 7.4. This work was carried out to perform a morphological analysis of the culture at various stages of the work.

In this stage, spherical or slightly oval-shaped cells with a uniform diameter can be observed. Their coloration is characterized by an intense green hue, due to the presence of photosynthetic pigments. Regarding cellular organization, some cells appear isolated while others tend to aggregate into more or less compact clusters. Trying to give an interpretation regarding their distribution, aggregations are advantageous for resisting light stress, promoting mutual protection.

Based on their morphology only, the hypothized genus is *Chlorella*.

4.5.2 Final phase of the experiment

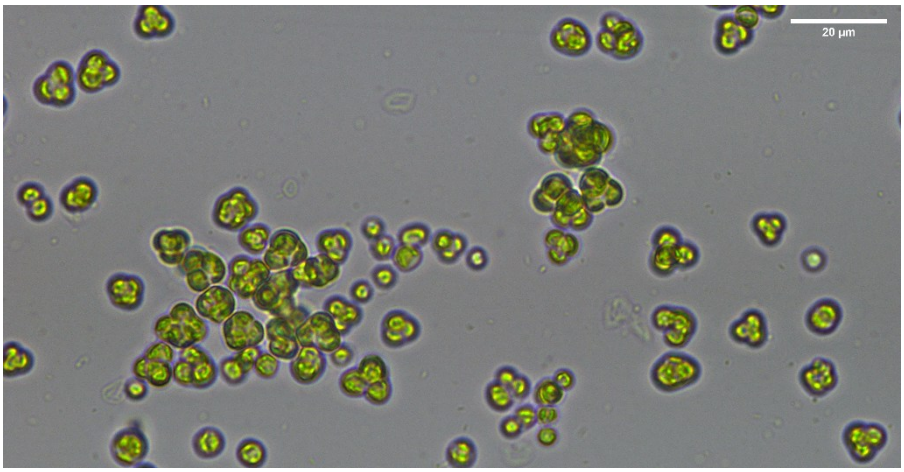

Fig. 30: Microscopic view (20x) of the culture at the final phase of the experiment.

At the end of the experiment, the microalgal culture was observed under the microscope. In this phase of the work, the culture had been maintained at 100% LED light intensity, 32°C, and pH 7.6 in the photobioreactor.

Cells displayed uniform circular shape bright green coloration, and many of them are undergoing division. Some were isolated while others formed aggregates. In some regions autospores are visible. In certain cells, the pyrenoid can be observed. Regarding cellular integrity, considering the end of the experiment, most cells appear intact, with no cellular fragments or lysed walls (a sign of cellular viability).

From the image, it appears that only one microalgal species (hypothetically genus *Chlorella*) was able to reproduce and remain viable despite the stressful conditions applied during the months of the experiment.

4.6 Pigment analysis

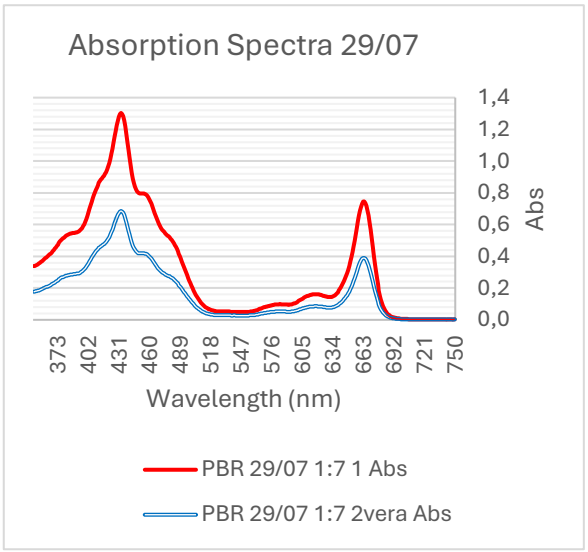

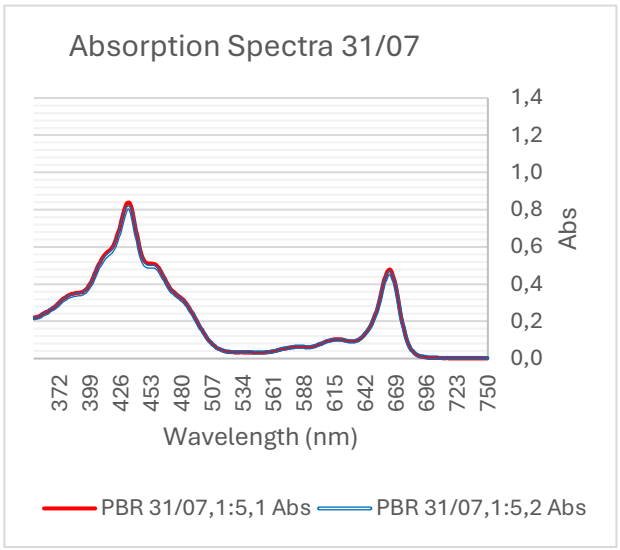

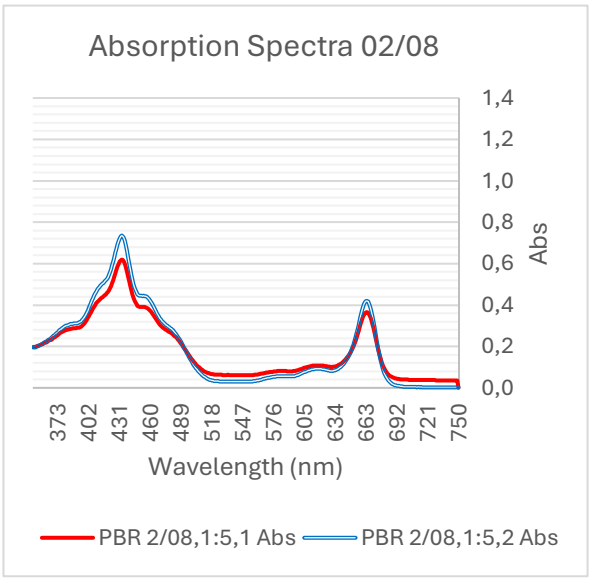

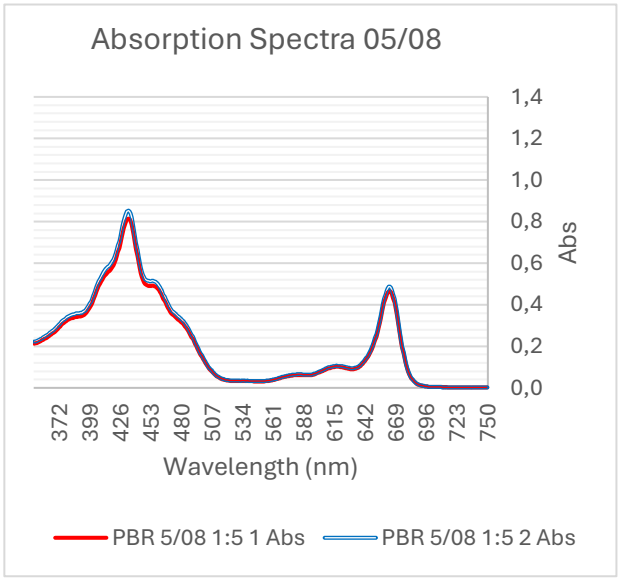

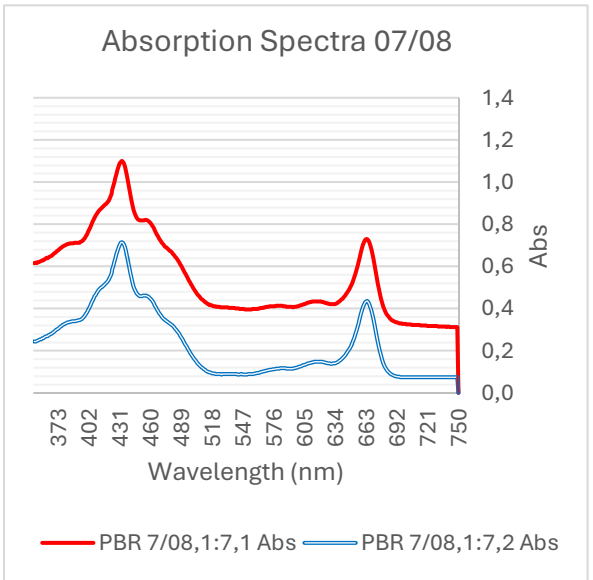

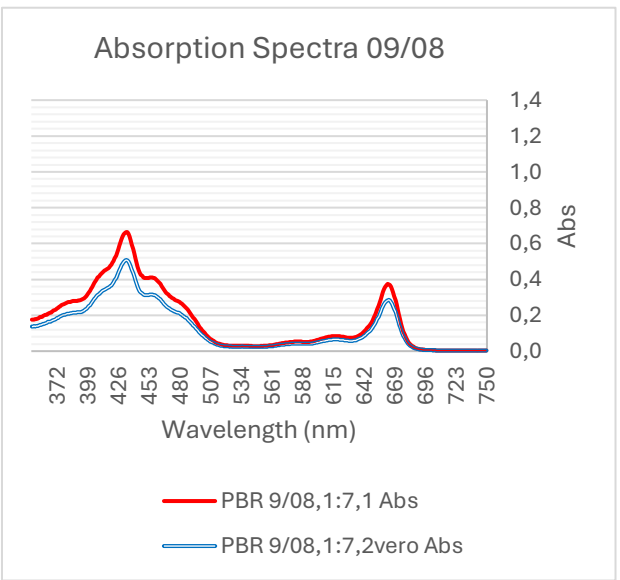

In these graphs, the absorption peaks of the pigments can be observed (carotenoids at 480 nm, chlorophyll a at 663 nm, and chlorophyll b at 646 nm) for the samples collected during the working phases (one before the semicontinuous dilution and one after the dilution).

Two main maxima can be observed for each sample: one at approximately 430 nm and one at approximately 663 nm, which can be attributed to chlorophyll a.

The absorption spectra of the samples 31/07 (day 138), 02/08 (day 140), and 05/08 (day 143) show very similar patterns, with overlapping curves. This indicates that the pigment composition and the ratios between chlorophyll a, chlorophyll b, and carotenoids are comparable between the samples. It may suggest that the physiological conditions of the samples analyzed are very similar, without significant variations.

In the graphs: 29/07 (day 136) and 07/08 (day 145), the positions of the peaks are the same, but a difference in height is observed, indicating a higher absorbance in sample 1 (collected before the dilution) compared to sample 2 (collected after the dilution). This suggests that the two samples have markedly different concentrations of photosynthetic pigments.

Despite the differences in intensity observed, most likely due to the dilution of the samples and the resulting decrease in biomass in the culture, the absorption spectra showed the same characteristic peaks of the pigments under study. The variations observed in pigment concentration can be attributed to the dilutions applied.

This work allowed for a deeper investigation not only into the quantification of pigment concentrations but also into the physiological state of the culture in the photobioreactor, as the presence and stability of the peaks reflect the functionality of the photosynthetic complexes and the culture's ability to capture light energy.

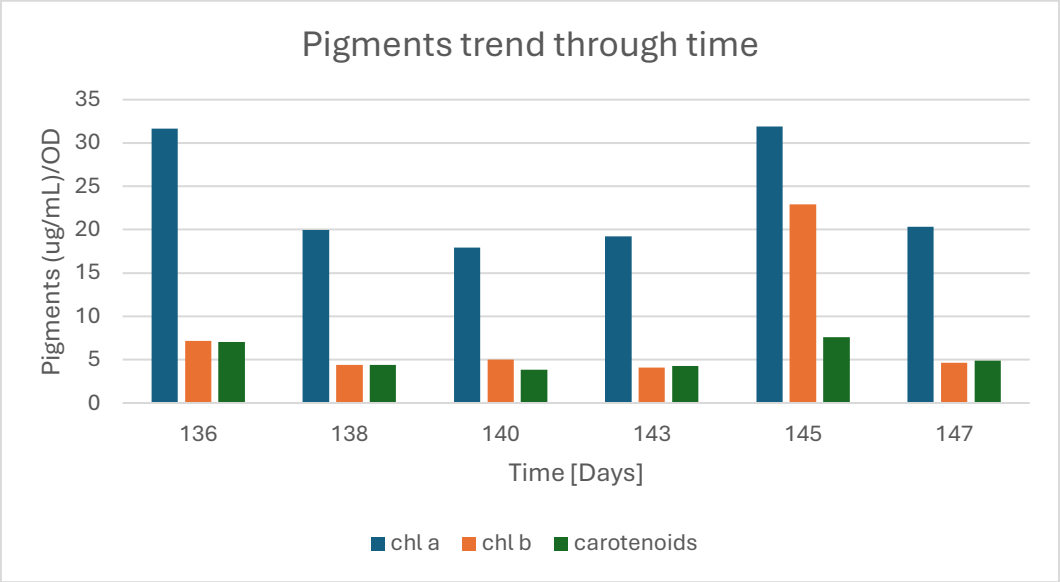

Fig. 31: pigment concentration (ug/mL)/OD trend of the samples.

Fig. 31 shows the time course of the normalized concentrations of chlorophyll a, chlorophyll b, and carotenoids (expressed as µg/mL/OD) in the samples collected between day 136 and day 147.

Discussing the results, chlorophyll a (blue) appears as the most abundant pigment, in line with its central role in photosynthesis. The values range between ~18 and ~32 µg/mL/OD. Two maxima can be observed on days 136 and 145, while in the intermediate days the values are lower (~18–20 ug/mL/OD).

Chlorophyll b (orange) shows greater variability compared to the other pigments, with a pronounced peak exceeding 20 µg/mL/OD on day 145. This fluctuation could be related to adaptive changes in the culture.

Carotenoids (green), on the other hand, display a more stable trend, confirming their mainly protective function, associated with a photoprotective role.

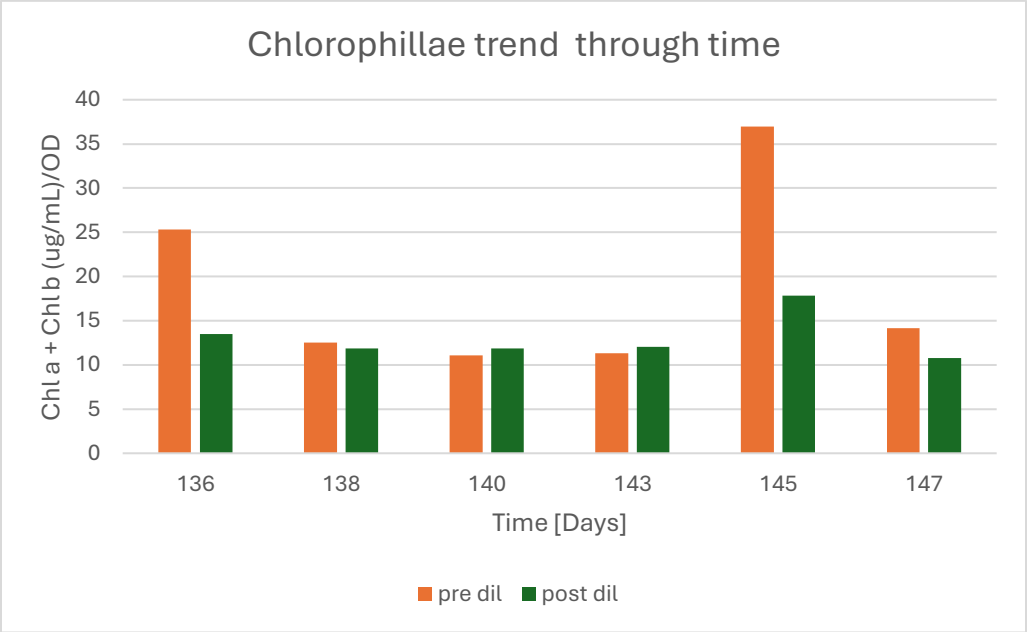

Fig. 32: Total chlorophyll (a+b) through time.

Fig. 32 illustrates the trend of total chlorophyll (a+b) on the sampling days, both before and after each semicontinuous dilution, as indicated.

The aim of this analysis was to evaluate the photosynthetic capacity, and the amount of biomass present during the sampling days, thereby providing further insight into the overall state of the culture.

In general, chlorophyll concentrations in the pre-dilution phases were higher compared to the corresponding post-dilution values, indicating pigment accumulation during growth prior to sampling.

After dilution, the values decreased, reflecting a reduction in cell density/pigments per unit volume.

On days 138, 140, and 143, the pre- and post-dilution values appeared more similar, suggesting a balance between chlorophyll accumulation and the effect of dilution. A maximum peak was recorded on day 145 during the pre-dilution phase, followed by a significant decline post-dilution.

This may indicate an initial overproduction of biomass. Immediately after dilution, the cells rapidly rebalanced pigment concentration in relation to a more balanced biomass growth within the photobioreactor.

4.7 Analysis of DNA extraction

	ID	Nanodrop [ng/µL]	A260/280	A260/230	Amount ng	µl	H_2O Dnase free	Vol. finale µl
B	29_07	17,2	2,293	1,502	300	17,4	2,6	20
A	31_07	21,05	1,995	1,589	400	19,0	1,0	20
B	02_08	14,85	2,339	1,084	250	16,8	3,2	20
B	05_08	16,55	2,122	1,085	300	18,1	1,9	20
B	07_08	12,75	2,04	0,766	250	19,6	0,4	20
B	09_08	18,85	2,327	0,873	350	18,6	1,4	20
B	27_08	57,5	1,99	1,882	1000	17,4	2,6	20
A	03_09	28,65	2,025	1,422	500	17,5	2,5	20
A	B12_09	10	2,027	1,599	200	20,0	0,0	20
A	P12_09	44,9	2,027	1,599	800	17,8	2,2	20
B	16_09	51,4	1,977	1,813	1000	19,5	0,5	20

Table 8: Analysis of DNA extraction in samples before (A) and after (B) dilutions.

Legend

ID: Sample identity (sampling date).

Nanodrop [ng/µL]: DNA concentration measured with the spectrophotometer.

A260/280: Ratio between absorbance at 260 nm and 280nm.

A 260/230: Ratio indicating contamination from salts or organic solvents.

Amount ng: Total amount of DNA extracted in ng.

µL: Volume of the sample analyzed.

H_2O DNase free: Volume of DNase – free water used to adjust the sample to the final volume.

Vol. finale µL: Final normalized volume of 20µL (standard for sequencing submission).

It can be observed that all samples reached the minimum concentration threshold (≥10 ng/µL) and are therefore suitable for the subsequent amplification and sequencing step, aimed at identifying the species present.

5 CONCLUSION

This work is intended to lay the foundation for future studies, shedding further light on the survival and reproductive capacities of microalgal species adapted to extreme environments, such as arid soils.

The experiments carried out in the photobioreactor showed that microalgae can persist under prolonged stress conditions, although with limitations related to adhesion phenomena and culture stability.

The results obtained may serve as a basis for completing the work through DNA sequencing and the identification of species by means of metabarcoding analysis. In this way, it will be possible to verify whether the observed dominance of *Chlorella* spp. is confirmed at the molecular level and to understand more precisely which species among those present have adapted to pH stress, light intensity, nutrient concentration, and temperature during the months of cultivation. This would directly address the fourth hypothesis formulated in this thesis.

More broadly, this work highlights an aspect often underestimated: the importance of investigating soils and the vast diversity of microorganisms that inhabit them. Understanding their ability to adapt and survive under extreme conditions is not only relevant for biodiversity knowledge but also essential for predicting their potential responses to ongoing climate change.. Moreover, essential ecosystem services for human development (such as soil fertility, biomass production, and food supply) largely depend on the abundance and composition of soil microorganisms, including fungi, bacteria, and microalgae. For this reason, it is crucial to understand how climate change affects microbial species in these environments. Yet, current knowledge on these organisms remains limited, as they are poorly represented in global databases.

The work carried out in the photobioreactor was fundamental for obtaining initial data under conditions that simulate industrial conditions. Cultivating extremophilic microalgae at large scale is particularly relevant because of their wide range of applications from dietary supplements to biofuel production, and organic fertilizers. Their ability to produce high levels of carotenoids is particularly relevant for biotechnological applications, especially in the cosmetic and pharmaceutical sectors. In conclusion, this

thesis confirms that extremophilic microalgae can withstand prolonged stress in controlled cultivation, partially supporting the hypotheses formulated at the beginning of the work. It also opens the way to further studies integrating long-term cultivation with metabarcoding-based molecular analyses. This dual ecological and applied perspective underlines the potential of desert microalgae both as a model for understanding resilience in extreme environments and as a resource for the development of a sustainable and circular bioeconomy.

6 BIBLIOGRAFY

1. *Evolution of Photobioreactors: A Review based on Microalgal Perspective*. **Ahmad, I., Abdullah, N., Koji, I., Yuzir, A., & Eva Muhammad, S.** 2021, IOP Conference Series: Materials Science and Engineering.

2. *Photobioreactor configurations in cultivating microalgae biomass for biorefinery*. **Regina Barboza-Rodríguez, Rosa M. Rodríguez-Jasso, Gilver Rosero-Chasoy, Miriam L. Rosales Aguado, Héctor A. Ruiz,.** 2024, Bioresource Technology.

3. *Effetto del rapporto di riciclo in fotobioreattori in continuo per la coltivazione di arthrospira maxima: composizione della biomassa e ottimizzazione del consumo di acqua e nutrienti*. **A.R, Colta.** 2023, Università degli Studi di Padova.

4. *The role of microalgae in the bioeconomy*. **Fernández FGA, Reis A, Wijffels RH, Barbosa M, Verdelho V, Llamas B.** 2021, New biotechnology.

5. *Photosynthetic recovery following desiccation of desert green algae (Chlorophyta) and their aquatic relatives*. **Gray, D. W., Lewis, L. A., & Cardon, Z. G.** 2007, Plant, cell & environment.

6. *Spirulina for the food and functional food industries*. **Lafarga, T., Fernández-Sevilla, J. M., González-López, C., & Acién-Fernández, F. G.** 2020, Food research international.

7. *Biogeography of global drylands*. **Maestre, Fernando T. and Benito, Blas M. and Berdugo, Miguel and Concostrina-Zubiri, Laura and Delgado-Baquerizo, Manuel and Eldridge, David J. and Guirado, Emilio and Gross, Nicolas and Kéfi, Sonia and Le Bagousse-Pinguet, Yoann and Ochoa-Hueso, Raúl and.** 2021, New Phytologist.

8. *Extremophile Microalgae: the potential for biotechnological application*. **Malavasi, Veronica and Soru, Santina and Cao, Giacomo.** 2020, Journal of Phycology.

9. *Recent Advances in Microalgal Bioactives for Food, Feed, and Healthcare Products: Commercial Potential, Market Space, and Sustainability*. **M U N, Mehar JG, Mudliar SN, Shekh AY.** 2019, Comprehensive reviews in food science and food safety.

10. *Biotechnological applications of extremophiles, extremozymes and extremolytes*. **Raddadi N, Cherif A, Daffonchio D, Neifar M, Fava F.** 2015, Applied microbiology and biotechnology.

11. *Polyphasic evaluation of key cyanobacteria in biocrusts from the most arid region in Europe*. **Roncero-Ramos B, Muñoz-Martín MÁ, Chamizo S,**

Fernández-Valbuena L, Mendoza D, Perona E, Cantón Y, Mateo P. 2019, PeerJ.

12. *I deserti e il rischio desertificazione.* **M, Sciortino.** 2021, Focus.

13. *Commercial applications of microalgae.* **Spolaore P, Joannis-Cassan C, Duran E, Isambert A.** 2006, Journal of bioscience and bioengineering.

14. *Cultivation in industrially relevant conditions has a strong influence on biological properties and performances of Nannochloropsis gaditana genetically modified strains.* **Perin, G, et al.** 2017, ALGAL RESEARCH.

15. **European Commission and Joint Research Centre and Vazquez Calderon, F and Sanchez Lopez, J.** *An overview of the algae industry in Europe. Producers, production systems, species, biomass uses, other steps in the value chain and socio-economic data.* 2022.

16. **Zuccaro, Gaetano and Yousuf, Abu and Pollio, Antonino and Steyer, J-P.** Microalgae Cultivation Systems. *Microalgae Cultivation for Biofuels Production.* 2019.

17. **Maestre, F. T.** *The BIODESERT survey: Assessing the impacts of grazing and climate change in global drylands.* Rey Juan Carlos University. 2017.

18. **Belnap, J.** *Encyclopedia of Soils in the Environment.* s.l. : Daniel Hillel, 2005.

19. **Perrone, C., Felicini, G.P.** I cianobatteri. [book auth.] G., Abbate, G., Forni, C Pasqua. *Botanica generale e diversità vegetale.* 2019.

20. *Increasing aridity reduces soil microbial diversity.* **Maestre, F. T., Delgado-Baquerizo, M., Jeffries, T. C., Eldridge, D. J., Ochoa, V., Gozalo, B., Quer, J. L., García-Gómez, M., Gallardo, A., Ulrich, W., Bowker, M. A., Arredondo, T., Barraza-Zepeda, C., Brank, D., Florentino, A., Gaitán, J., Gutiérrez, J.** Washington, D.C., USA : National Academy of Sciences, 2015, Vol. 112. 10.1073/pnas.1516684112.

21. **A.R, Wellburn.** The spectral determination of chlorophylls a and b, as well as total carotenoids, using various solvents with spectrophotometers of different resolution. *Journal of Plant Physiology.* 1994, Vol. 144, 3.

22. **Bischoff, H.W. & Bold, H.C.** Phycological studies IV. Some soil algae from Enchanted Rock and related algal species. Austin, Texas, USA : s.n., 1963. 6318.

7 APPENDIX

Table summarizing all daily measurements recorded during the first experiment.

Dates	Days	Measure 710nm	Measure 710nm	Measure 710nm	Average OD	pH	LED	T
18/01/2024	0	0,028	0,017	/	0,02	6,2	1	24,4
19/01/2024	1	/	/	/	0,18	6,3	1	24,4
22/01/2024	4	/	/	/	0,09	6,7	1	22,8
23/01/2024	5	0,148	0,218	/	0,32	6,8	1	23
31/01/2024	13	0,128	0,051	/	0,33	6,4	2	24,4
05/02/2024	18	0,252	0,363	0,333	0,39	6,7	2	24,2
09/02/2024	22	0,313	0,349	0,326	0,09	6,3	3	26,5
16/02/2024	29	0,373	0,384	0,398	0,07	6,5	3	26,4
16/02/2024	29	0,107	0,088	0,073	0,14	6,5	3	26,4
22/02/2024	35	0,077	0,055	0,073	0,29	7,7	10	27,1
27/02/2024	40	0,18	0,15	0,1	0,12	7,2	10	28
29/02/2024	42	0,252	0,31	0,307	0,02	7	12	28,9
04/03/2024	46	0,101	0,114	0,134	0,18	7,5	12	26,8

Table 9: data collected during the first experiment.

Table summarizing all daily measurement and conditions to which the culture was subjected during the second experiment.

Dates	Days	Average OD 750nm	pH	T	LED
27/03/2024	14	0,0765	7,5	26	7
03/04/2024	21	0,562	7,1	26,9	9
05/04/2024	23	0,6605	7,1	29,6	15
08/04/2024	26	0,808	7,1	31,3	15
11/04/2024	29	1,072	7,1	26,3	15
11/04/2024	29	0,19	7,1	26,3	25
15/04/2024	32	0,91	7,1	26,2	25
17/04/2024	34	1,34	7,1	26,2	25
19/04/2024	36	1,41	7,1	26	25
22/04/2024	39	1,72	7,1	25	25
24/04/2024	41	1,66	7,1	25,7	25
29/04/2024	46	1,65	7,1	27,2	25
29/04/2024	46	0,689	7,1	27,2	25
02/05/2024	49	1,70	7,1	27,4	25
03/05/2024	50	1,04	7,1	26,8	25
06/05/2024	53	1,16	7,2	27,2	25
08/05/2024	55	1,35	7,2	26,5	25
10/05/2024	57	1,79	7,3	29,9	25
13/05/2024	60	2,04	8,1	25,6	25
14/05/2024	61	2,40	7,4	28,1	25
14/05/2024	61	2,53	7,4	28,1	25
15/05/2024	62	2,142	7,5	27,5	25
16/05/2024	63	2,06	7,3	27,8	25
16/05/2024	63	1,498	7,3	27,8	25
20/05/2024	67	2,17	7,2	28,4	50
20/05/2024	67	1,254	7,2	28,4	50
21/05/2024	68	1,618	7,1	28,5	50
23/05/2024	70	1,89	7,1	28,5	50
24/05/2024	71	2,509	7,1	29,5	70

24/05/2024	71	1,856	7,1	29,5	70
28/05/2024	74	2,694	7,2	27,2	43
28/05/2024	74	1,813	7,2	27,2	114
30/05/2024	76	2,182	7,3	29,7	76
03/06/2024	80	2,795	7,3	31	64
03/06/2024	80	1,614	7,3	31	64
05/06/2024	82	2,282	7,2	29,8	72
07/06/2024	84	2,756	7,6	30	73
07/06/2024	84	1,923	7,5	30	73
10/06/2024	87	2,6745	7,4	29,6	69
11/06/2024	88	2,735	7,6	30	84
11/06/2024	88	1,844	7,6	30	84
14/06/2024	91	2,399	7,6	30	94
19/06/2024	96	3,221	7,8	30,6	100
19/06/2024	96	2,277	7,8	30,6	100
21/06/2024	98	2,615	7,7	30,1	79
25/06/2024	102	3,239	7,8	29,8	88
25/06/2024	102	2,128	7,6	29	99
	104	PHOTOPERIOD SETUP 16/8			
28/06/2024	105	2,66	7,7	30,1	98
28/06/2024	105	2,175	7,6	29,6	99
05/07/2024	112	3,411	7,9	29,6	90
05/07/2024	112	2,262	7,6	30	98
10/07/2024	117	3,127	7,8	29,6	67
10/07/2024	117	2,048	7,7	29,5	80
17/07/2024	124	2,644	10,8	30	78
17/07/2024	124	2,398	8,3	29,8	73
22/07/2024	129	3,093	7,9	29,4	67
22/07/2024	129	2,446	7,8	29,2	75
24/07/2024	131	2,614	7,7	29,3	68
26/07/2024	133	2,929	7,9	29,8	94
26/07/2024	133	2,149	7,7	29,2	97
29/07/2024	136	2,725	7,8	29,9	88
29/07/2024	136	2,152	7,7	29,2	84
31/07/2024	138	2,566	7,9	31,4	96

31/07/2024	138	2,03	7,9	30,9	93
02/08/2024	140	2,383	7,9	30,7	75
02/08/2024	140	1,884	7,7	30,1	81
05/08/2024	143	2,699	7,9	30,7	87
05/08/2024	143	2,098	7,8	29,9	90
07/08/2024	145	2,589	8	30,8	100
07/08/2024	145	2,016	7,8	29,8	100
09/08/2024	147	2,439	7,4	27,9	80
09/08/2024	147	1,808	7,3	27,7	80
13/08/2024	151	2,15	7,3	30,5	100
13/08/2024	151	1,799	7,4	29,2	100
16/08/2024	154	2,24	7,3	32,6	100
16/08/2024	154	1,447	7,4	32,3	100
22/08/2024	160	2,05	7,4	32,4	100
22/08/2024	160	1,463	7,4	29,9	100
27/08/2024	165	1,766	7,6	32,5	100
27/0872024	165	1,428	7,6	31,5	100
03/09/2024	172	2,13	7,5	33	100
03/09/2024	172	1,811	7,5	32,3	100
12/09/2024	181	2,217	7,7	32,3	100
12/09/2024	181	1,706	7,6	32	100
16/09/2024	185	2,673	8	31,7	100
16/09/2024	185	2,12	7,9	30,2	100
18/09/2024	187	2,62	8,7	32,7	100
18/09/2024	187	2,05	8,4	31,5	100
20/09/2024	189	2,31	8,9	32,2	100
20/09/2024	189	1,91	8,9	32,1	100
23/09/2024	192	1,93	8,9	31,6	100
23/09/2024	192	1,30	8,9	32,1	100
25/09/2024	194	1,49	7,5	32,4	100
25/09/2024	194	1,15	7,6	31,7	100

Table 10: Data collecterd during the second experiment.

Table summarizing the biomass dry weight values on the sampling days. The first value (highlighted in gray) indicates the concentration in g/L before dilution, while the second value represents the calculated concentration after dilution. As mentioned earlier, at the end of each dilution the aim was to maintain a value of approximately 1 g/L.

Days	Biomass $_{dry}$ (g/L)	dilution (mL)
63	1,6	400
	0,775	
67	1,4	400
	0,98	
71	1,48	400
	0,76	
74	0,58	400
	0,64	
80	1,02	300
	0,98	
84	1,44	300
	0,88	
88	1,46	400
	0,88	
96	1,9	400
	1,36	
102	1,74	500
	1,02	
105	1,36	400
	0,86	
112	1,79	500
	1,04	
117	1,66	500
	0,96	
124	1,62	300
	1,28	
129	1,76	400
	1,3	
133	1,44	400
	0,96	
136	1,46	300
	1,1	

138	1,4	300
	1,1	
140	1,16	300
	0,88	
143	1,2	300
	0,96	
145	1,38	300
	1,02	
147	1,34	300
	1,04	
151	1,3	300
	0,96	
154	1,26	300
	0,66	
160	1,16	300
	0,82	
165	0,8	300
	0,58	
172	1,04	300
	0,82	
181	1,24	300
	0,88	
185	1,56	300
	1,1	
187	1,82	300
	1,8	
189	1,66	300
	1,2	
192	1,48	300
	1,24	
194	1,08	300
	0,74	

Table 11: Summarizing the biomass dry weight values on the sampling days.

	29/07/2024 (136)		31/07/2024 (138)		02/08/2024 (140)		05/08/2024 (143)		07/08/2024 (145)		09/08/2024 (147)	
Wavelenghts nm	Before dil	After dil	Before dil	After dil	Before dil	After dil	Before dil	After dil	Before dil	After dil	Before dil	After dil
663	0,74	0,39	0,48	0,46	0,37	0,42	0,46	0,49	0,73	0,43	0,37	0,28
646	0,26	0,14	0,17	0,16	0,15	0,15	0,16	0,17	0,48	0,2	0,13	0,1
480	0,51	0,27	0,32	0,32	0,26	0,28	0,32	0,33	0,67	0,32	0,27	0,21
Chl a conc ug/mL	8,0714	4,2446	5,2313	5,0224	3,9735	4,5735	5,0224	5,3513	7,2672	4,538	4,0357	3,049
Chl b conc ug/ml	1,7916	1,006	1,1902	1,08	1,3114	1,0674	1,08	1,1414	6,412	2,0576	0,8958	0,7116
Chl+C conc ug/mL	1,795593	0,942741	1,116697	1,132977	0,860695	0,973516	1,1329768	1,163751	1,809812	0,999245	0,959021	0,744249
OD750	2,725		2,566		2,383		2,699		2,589		2,439	
Dilution factor (DMF)	7		5		5		5		7		7	
OD750 in DMF	0,389285714		0,5132		0,4766		0,5398		0,369857143		0,348428571	
Chl a conc (ug/mL)/ OD	20,73387	10,90356	10,19349	9,786438	8,33718	9,596097	9,3041867	9,913486	19,64867	12,2696	11,58257	8,750718
Chl b conc (ug/mL)/ OD	4,602275	2,58422	2,319174	2,104443	2,751574	2,239614	2,000741	2,114487	17,33642	5,563229	2,570972	2,042312
Car conc (ug/mL)/OD	4,612532	2,421721	2,175949	2,207671	1,805906	2,042626	2,0988825	2,155893	4,893273	2,701705	2,752417	2,136015

Table 12: Daily measurements of optical density (OD), pigment concentrations (Chl a, Chl b, carotenoids), and dilution factors of the culture during the second experiment. For each sampling day, values before and after dilution are reported.

RINGRAZIAMENTI

Ringrazio il mio relatore professor Francesco Dal Grande, che mi ha permesso di intraprendere questo interessante tirocinio, dandomi la possibilità di lavorare col suo gruppo di lavoro arricchendo ancora di più il mio bagaglio culturale.

Ringrazio Veronica, che mi ha aiutato ed insegnato con pazienza molto in questi mesi, stuzzicando ancora di più la mia curiosità verso questa ricerca, rendendosi sempre disponibile a consigli e supporto nel lavoro.

Ringrazio il gruppo “Plants Lab” in particolare Eleonora, che mi ha insegnato e seguito con molta pazienza e gentilezza durante i miei mesi al Vallisneri.

Ringrazio la mia famiglia, per avermi permesso di intraprendere questo percorso, per avermi ascoltato e spronato. Se tutto questo oggi è possibile è anche grazie a loro.

Ringrazio Andrea, è stato un faro di luce per me in un periodo particolarmente buio del mio percorso. È stato un collega, un amico, un coach. Una persona che io considero rara da incontrare. Se non avessi intrapreso questo progetto non lo avrei mai conosciuto. Non posso che essere più grata alla vita per regalo che mi ha fatto.

Ringrazio Pietro, per essere stato a mio fianco e di supporto durante gli ultimi esami e scrittura della tesi. È stato per me un punto di riferimento, con la sua sensibilità e dolcezza mi ha trasmesso molta calma e fiducia per affrontare questi ultimi mesi. Sono molto grata di avere una persona come lui al mio fianco.

E per ultimo, ma non per importanza, ringrazio i miei amici più cari, per essere sempre stati i miei sostenitori numero uno, per avermi spronato ed incoraggiato, facendomi sempre sentire in grado di affrontare qualsiasi cosa. La fine di questo percorso che a me piace chiamare “viaggio”, non è solo un traguardo importante, è anche una rivincita verso me stessa, per le mie insicurezze e paure di non essere all’altezza e di non farcela. È anche un riscatto verso chi negli anni mi diceva che davvero non ce l’avrei mai fatta. Fiera di essere una biologa e di essere la persona che sono.

Brava Laura.